CONSTANT-PRESSURE LAMINAR MIXING OF A SHEAR LAYER WITH A QUIESCENT FLUID

Thesis by

Chia-Chun Chao

In Partial Fulfillment of the Requirements

For the Degree of

Aeronautical Engineer

California Institute of Technology

Pasadena, California

1968

(Submitted February 20, 1968)

ACKNOWLEDGMENTS

The author wishes to express his sincere gratitude to Prof. Lester Lees and Dr. Toshi Kubota for their constant help and encouragement throughout the course of this investigation. He would also like to thank Mrs. Virginia Conner for typing the manuscript.

This research was sponsored by the U. S. Air Force Office of Scientific Research under Contract No. AF 49(638)-1298.

ABSTRACT

The constant-pressure laminar mixing of an initial shear layer with a quiescent fluid is studied theoretically. The line of singularities at the starting point is removed by abandoning the conventional restriction that the dividing streamline must coincide with the x-axis. Instead, the shape of this streamline in the "near-field" is determined by properly matching inner and outer flow regions so as to cancel any additional induced normal velocity and pressure disturbances in the outer flow. The "far-field" is obtained by applying the momentum integral technique beginning with the profiles determined by the near-field solution some distance downstream of the start of mixing. Universal functions are obtained that enable the progress of the mixing process to be followed both for a Blasius initial profile and an initial profile with a finite slip.

TABLE OF CONTENTS

LIST OF TABLES

LIST OF FIGURES

LIST OF SYMBOLS

x_1 , y_1	rectangular coordinates with x_1 along free stream
p	static pressure
h	static enthalpy
u_1 , v_1	velocity components parallel and normal to the free stream flow
u, v	normalized velocity components of u_1 and v_1 respectively $\left(u = \frac{u_1}{U} , \quad v = \frac{u_1}{U}\sqrt{R}\right)$
U	free stream velocity
$U_o(y)$	initial velocity profile at $x = 0$ or $x_1 = L$
R	Reynolds number $\left(\frac{UL}{\nu_\infty}\right)$
L	length from leading edge to the sharp corner
X, Y	Stewartson's transformed coordinates
ψ	stream function
μ	viscosity
ν	kinematic viscosity
T	absolute temperature
ρ	density
M	Mach number
S	total enthalpy, $h + \frac{1}{2} u_1^2$
H	normalized total enthalpy $\left(\frac{S}{H_\infty}\right)$
x, y	normalized Stewartson's coordinates $x = \frac{X-L}{L}$ $y = \frac{Y}{L}\sqrt{R}$
$f(\psi)$	normalized stream function
$f(\xi, \eta)$	normalized stream function in ξ, η plane
ξ, η	transformed inner variables $\xi = x^{1/n}$, $\eta = \frac{y}{\xi}$
$f_r(\eta)$	coefficient of ξ^{m+r} term in the inner expansion of stream function

LIST OF SYMBOLS (Cont'd)

γ	$\frac{C_p}{C_v}$
a	slope of the Blasius velocity profile at the surface of plate ($a = 0.332$)
A, B, C, D	coefficients of the initial velocity profile in terms of a power series
a, b	coefficients of inner stream function in terms of a power series
δ_1	shear layer thickness in region (1)
δ_2	shear layer thickness in region (2)
$f(\eta), g(\xi)$	normalized velocity profiles in layer (1) and (2)

Superscripts

*	properties along dividing streamline
'	first derivative of a function with its variable

Subscripts

1	dimensional quantities
w	properties at the surface of the plate
s	properties of finite slip initial velocity case
b	properties of the base region
∞	free stream properties

I. INTRODUCTION

In recent years considerable effort has been devoted to the study of wake flow problems. Since the wake region is very complex it has been found useful to divide this region into various important subregions, such as the "outer inviscid wake" generated by the bow shock, and the "inner viscous wake" near the axis formed by the coalescence of the free shear layers shed from the body (Figure 1). When the inner wake becomes turbulent it can diffuse into the outer wake and swallow it completely before the outer wake has cooled appreciably. This phenomenon has been investigated by Lees and Hromas[1] and others.

We can also make a useful distinction between the "near wake", which includes the recirculating base flow bounded by the free shear layers, the recompression region and the wake shock--and the "far wake", in which some form of self-similar flow has been established. The present study is concerned mainly with the mixing problem in the free shear layers, and, more specifically, with the portion of the free shear layers near the base and not too close to the neck in which the static pressure is virtually constant.

Charters[2] and Thomas' shadowgraph of spheres indicated that for Mach numbers greater than 3 the flow in the base region and free shear layers is laminar at least up to the neck over a wide range of Reynolds numbers. Chapman[3] first investigated the constant pressure free shear layer theoretically and obtained a similar solution by considering the simple case of zero initial boundary layer thickness. In most cases a laminar boundary layer of appreciable thickness exists

at the point where mixing begins, and Chapman's similar solution can only apply to the region "far downstream", where the mixing layer has already swallowed the original boundary layer.

Laminar mixing at constant pressure with a finite initial boundary layer thickness in a compressible stream with a dead-air region has been studied by several investigators. Kubota and Dewey[4] and Reeves[5] used a momentum integral technique to describe the non-similar growth of the constant pressure-laminar free shear layer with finite initial thickness. They divided the shear layer into two parts, one above and one below the dividing streamline. Denison and Baum[6] introduced a shear function and employed an implicit finite difference method to find the shear layer flow field, starting from a Blasius initial velocity profile. Toba[7] solved the same problem by applying the method of inner and outer expansions for the "near field" and a perturbed asymptotic solution for the "far field".* He represented the initial velocity profile as a polynomial with finite slip. But his outer solution has a line of singularities at the starting point, where no singularity should occur in the outer solution.

The purpose of the present investigation is to remove the line of singularities at the starting position by permitting the dividing streamline to deflect away from the conventionally assumed straight line, in order to cancel the pressure disturbances in the outer solution. Matching of inner and outer regions is used to obtain the proper initial development of the mixing layer into a non-uniform vorticity field.

---

* The terms "near field" and "far field" are based on a non-dimensional parameter of the form $\nu(x_1-L)/\theta_o^2$, which measures the degree of mixing.

The "far field" is obtained by applying the momentum integral technique beginning with the profiles determined from the near-field solution some distance downstream of the start of mixing. If the distance from the base of the body to the rear stagnation point is within the region of convergence of the near field solution, the momentum integral solution becomes unnecessary.

In the case of the flat wall (Figure 2) the initial profile is taken to be a Blasius profile. But in the case of a slender blunt-based body at hypersonic speeds the boundary layer on the body surface undergoes a rapid expansion around the sharp corner of the base (Figure 3). Thus the initial velocity profile is no longer of Blasius type. A modified profile of arbitrary shape in terms of a polynomial with a finite slip at the corner is used by Toba and also in the present study. Universal functions are obtained that enable the progress of the constant pressure mixing process to be followed in both of these interesting cases.

II. FORMULATION OF THE PROBLEM

When a two-dimensional stream leaves a flat surface at a sharp corner, it will start to mix with the quiescent fluid at the base (Figure 2). The flow is assumed to be laminar and the pressure in the quiescent fluid is constant. The coordinate system is chosen so that the x_1-axis is in the direction of the outer inviscid flow and y_1 lies in the perpendicular direction; the origin is at the leading edge of the semi-infinite body (Figure 2).

The boundary layer approximation is assumed to be valid everywhere in the mixing region except at the point $x_1 = L$, $y_1 = 0$, where there is a singularity. Thus $\frac{\partial p}{\partial y} = 0$ to the first order. Since $p = p_\infty$ everywhere in the quiescent fluid it follows that the static pressure must be uniform in the outer inviscid flow as well, and the additional velocity component in the y_1-direction induced by mixing must vanish as $y_1 \to \infty$. This boundary condition takes the place of the usual condition that the dividing streamline coincides with the x_1-axis.

The boundary conditions are as follows:

$0 < x_1 < L$	$u_1 = U_o(y)$		$y_1 > 0$
	$u_1 = 0$		$y_1 < 0$
	$h = h_o(y)$		$y_1 > 0$
	$h = h_w$		$y_1 < 0$
$x_1 > L$	$u_1 \to U$, $h \to h_\infty$		$y_1 \to \infty$
	$u_1 \to 0$, $h \to h_c$		$y_1 \to -\infty$
	$p \to p_\infty$	as	$y_1 \to \pm\infty$

The fluid is assumed to be homogeneous and no chemical reactions or ionizations occur. Prandtl number is unity and viscosity μ is linearly proportional to absolute temperature. Body forces are neglected.

The basic conservation equations can be written as

$$\frac{\partial}{\partial x_1}(\rho u_1) + \frac{\partial}{\partial y_1}(\rho v_1) = 0 \tag{1}$$

$$\rho u_1 \frac{\partial u_1}{\partial x_1} + \rho v_1 \frac{\partial u_1}{\partial y_1} = \frac{\partial}{\partial y_1}\left(\mu \frac{\partial u_1}{\partial y_1}\right) \tag{2}$$

$$\rho u_1 \frac{\partial h}{\partial x_1} + \rho v_1 \frac{\partial h}{\partial y_1} = \frac{\partial}{\partial y_1}\left(\frac{k}{g c_p} \frac{\partial h}{\partial y_1}\right) + \mu\left(\frac{\partial u_1}{\partial y_1}\right)^2 \tag{3}$$

By applying the Stewartson transformation

$$X = x_1 \qquad Y = \int_o^{y_1} \frac{\rho}{\rho_\infty}\, dy \quad , \tag{4}$$

introducing a stream function $\bar{\psi}$ such that

$$u_1 = \rho_\infty/\rho \; \frac{\partial \bar{\psi}}{\partial y_1}$$

$$v_1 = -\rho_\infty/\rho \; \frac{\partial \bar{\psi}}{\partial x_1}$$

and utilizing the relations [Eq. (4)]

$$\frac{\partial}{\partial x_1}\Big)_{y_1} = \frac{\partial}{\partial X} + \frac{\partial Y}{\partial x_1}\Big)_{y_1} \frac{\partial}{\partial Y}$$

$$\frac{\partial}{\partial y_1}\Big)_{x_1} = \frac{\rho}{\rho_\infty} \frac{\partial}{\partial Y}$$

the momentum equation [Eq. (2)] becomes

$$\frac{\partial \bar{\psi}}{\partial Y} \frac{\partial^2 \bar{\psi}}{\partial X \partial Y} - \frac{\partial \bar{\psi}}{\partial X} \frac{\partial^2 \bar{\psi}}{\partial Y^2} = \nu_\infty \frac{\partial^3 \bar{\psi}}{\partial Y^3} \tag{5}$$

or

$$u_1 \frac{\partial u_1}{\partial X} + \bar{v} \frac{\partial u_1}{\partial Y} = \nu_\infty \frac{\partial^2 u_1}{\partial Y^2} \tag{5a}$$

where $\bar{v} = -\left(\frac{\partial \bar{\psi}}{\partial X}\right)_Y$

In the same manner the equation for the total enthalpy $S = h + \frac{1}{2} u_1^2$, namely

$$\rho u_1 \frac{\partial S}{\partial x_1} + \rho v_1 \frac{\partial S}{\partial y_1} = \frac{\partial}{\partial y_1}\left(\mu \frac{\partial S}{\partial y_1}\right) \tag{6}$$

is transformed to

$$\frac{\partial \bar{\psi}}{\partial Y} \frac{\partial S}{\partial X} - \frac{\partial \bar{\psi}}{\partial X} \frac{\partial S}{\partial Y} = \nu_\infty \frac{\partial^2 S}{\partial Y^2} \tag{7}$$

or

$$u_1 \frac{\partial S}{\partial X} + \bar{v} \frac{\partial S}{\partial Y} = \nu_\infty \frac{\partial^2 S}{\partial Y^2} \tag{7a}$$

Nondimensionalize the above equations with proper reference quantities, as follows:

Let

$$u = \frac{u_1}{U} \qquad \psi = \frac{\bar{\psi}}{\sqrt{U L \nu_\infty}}$$

$$v = \frac{\bar{v}}{U}\sqrt{R} \qquad R = \frac{UL}{\nu_\infty}$$

$$x = \frac{X-L}{L} \qquad H = \frac{S}{H_\infty}$$

$$y = \frac{Y}{L}\sqrt{R}$$

Then equations (1), (5), (7) become

$$\frac{\partial u}{\partial x} + \frac{\partial v}{\partial y} = 0 \tag{8}$$

$$u \frac{\partial u}{\partial x} + v \frac{\partial u}{\partial y} = \frac{\partial^2 u}{\partial y^2} \tag{9}$$

$$u \frac{\partial H}{\partial x} + v \frac{\partial H}{\partial y} = \frac{\partial^2 H}{\partial y^2} \tag{10}$$

Equations (9) and (10) indicate that $H = A + Bu$ is a solution of the energy equation (10), where A and B are constants. This solution is admissible only if the initial and boundary conditions permit. The momentum equation (9) is now independent of the energy equation (10).

III. NEAR FIELD SOLUTION

Similar solutions for this kind of mixing problem exist only in two cases: (1) Chapman's model, with zero initial boundary layer thickness, in which the dividing streamline is assumed to lie along the x_1-axis and interaction effects are ignored; (2) mixing between a uniform shear flow and a fluid at rest. This problem has been investigated by Rott and Hakkinen[8]. For incompressible flow, their results show that no lateral displacement is induced at infinity because of the laminar mixing, provided that the dividing streamline is a cubic curve lying above the x axis. In the present case the vorticity in the outer flow is not a constant value as x increases; thus a similar solution for all x does not exist. A similar problem, the mixing in the wake behind a flat plate with initial Blasius velocity profile, was worked out by Goldstein[9]; in his case the flow is symmetric about the x_1-axis.

One expects that the initial discontinuity in vorticity at $x_1 = L$, $y_1 = 0$ is smoothed out by viscous action, and rapid variations in flow quantities are confined to a narrow "inner" layer near $y_1 = 0$. When the initial velocity profile at $x_1 = L$ is a Blasius profile this inner layer grows into a region of uniform vorticity at first. In that case it is well-known [see Goldstein (9)] that the thickness of the inner layer $\sim x^{\frac{1}{3}}$, and the proper normal distance in the inner layer is of the form $\eta = y/x^{\frac{1}{3}}$, where $x = x_1 - L$. On the other hand, when the initial velocity profile has a finite "slip", i.e. $u(L, 0) \neq 0$, the flow near the axis behaves locally like a Chapman flow initially, and the inner layer grows like $x^{\frac{1}{2}}$ at first. In this case the proper normal distance is $\eta = y/x^{\frac{1}{2}}$.

In all cases the outer viscous shear layer is unaffected at first outside of a thin sub-layer of thickness $\sim x^{\frac{1}{3}}$ (or $x^{\frac{1}{2}}$) and it continues to develop in the downstream direction as if the wall were still present. The inner flow is determined by imposing the conditions

$$\psi_{\substack{\text{INNER} \\ \eta \to \infty}} \quad \to \quad \psi_{\substack{\text{OUTER} \\ y \to 0}}$$

and

$$u_{\substack{\text{INNER} \\ \eta \to \infty}} \quad \to \quad u_{\substack{\text{OUTER} \\ y \to 0}} \quad ,$$

where the outer flow is determined for $x_1 > L$ by analytic continuation. Of course this representation of the near-field is only an asymptotic expansion valid "sufficiently near" the trailing edge.

(1) Blasius Initial Velocity Profile

In the thin sub-layer near the axis the normalized stream function is represented as follows:

$$\psi(x, y) = \xi^m f(\xi, \eta) \tag{11}$$

where $\xi = x^{1/n}$ $\qquad \eta = y/\xi$

$$u = \psi_y = \xi^{m-1} f_\eta$$

$$v = -\psi_x = -\frac{1}{n} \xi^{m-n} (mf + \xi f_\xi - \eta f_\eta)$$

$$\frac{\partial u}{\partial x} = \frac{1}{n} \xi^{m-n-1} [(m-1)f_\eta + \xi f_{\xi\eta} - \eta f_{\eta\eta}]$$

$$\frac{\partial u}{\partial y} = \xi^{m-2} f_{\eta\eta}$$

$$\frac{\partial^2 u}{\partial y^2} = \xi^{m-3} f_{\eta\eta\eta}$$

where m and n are constants to be determined. By substituting these relations into Eq. (9), the momentum equation becomes

$$\xi^{m-3}[f_{\eta\eta\eta} + \frac{1}{n}\xi^{m-n+1}(mff_{\eta\eta} - \{m-1\}f_{\eta}^{2} + \xi f_{\xi} f_{\eta\eta} - \xi f_{\xi\eta} f_{\eta})] = 0$$

In order to make the convection terms of the same order as the viscous term, we must have

$$m = n-1$$

Then

$$nf_{\eta\eta\eta} + mff_{\eta\eta} - (m-1)f_{\eta}^{2} + \xi f_{\xi} f_{\eta\eta} - \xi f_{\xi\eta} f_{\eta} = 0 \qquad (12)$$

In the region near the base of the body where x is small or ξ is small the new stream function $f(\xi, \eta)$ can be expanded in terms of a power series in ξ:

$$f(\xi, \eta) = f_{o}(\eta) + \xi f_{1}(\eta) + \xi^{2} f_{2}(\eta) + \text{----} + \xi^{r} f_{r}(\eta) + \text{---} \qquad (13)$$

By substituting (13) into (12) and making use of the fact that the sums of the coefficients of the individual powers of ξ must vanish identically, one has

$$\begin{aligned}
&nf_{o}''' + m f_{o} f_{o}'' - (m-1) f_{o}'^{2} = 0 \\
&nf_{1}''' + m f_{o} f_{1}'' - (2m-1) f_{o}' f_{1}' + (m+1) f_{o}'' f_{1} = 0 \\
&nf_{r}''' + m f_{o} f_{r}'' - (2m+r-2) f_{o}' f_{r}' + (m+r) f_{o}'' f_{r} \\
&\qquad = -\sum_{j=1}^{r-1} [(m+j) f_{j} f_{r-j}'' - (m+j-1) f_{j}' f_{r-j}'], \quad r \geq 2.
\end{aligned} \qquad (14)$$

The series expansion [Eq. (13)] is valid for small x or ξ (provided $n > 0$) and y should be of same order of ξ, so the solution is confined to a narrow layer near $y = 0$. One boundary condition at the lower

edge of this mixing layer is $u_1 = 0$, which corresponds to

$$f_o' = f_1' = f_2' = \text{----} = f_r' = 0 \qquad \text{as } \eta \to -\infty$$

Since the differential equations of $f_r(\eta)$ are third order, two additional boundary conditions are needed. They will be supplied by matching with the outer solution.

For small x the outer solution is determined by using a Taylor's series expansion of the Blasius solution for $x > 0$ or $x_1 > L$. For our present purposes the Blasius solution for flow past a flat plate can be written in terms of a power series for small Y:

$$\bar{\Psi} = \sqrt{\nu_\infty x_1 U}\left(\frac{a}{2}\zeta^2 - \frac{a^2}{2.5!}\zeta^5 + \frac{11}{4}\frac{a^3}{8!}\zeta^8 \text{-----}\right)$$

where

$$\zeta = Y\sqrt{\frac{U}{\nu x_1}} \qquad \zeta_o = Y\sqrt{\frac{U}{\nu L}} = y$$

Then the Taylor series expansions around $x = 0$ are

$$\bar{\Psi}_{OUTER} = \bar{\Psi}_o = (\bar{\Psi})_{x_1=0} + x_1 \frac{\partial \bar{\Psi}}{\partial x_1}\Big|_{x_1=0} + \frac{x_1^2}{2!}\frac{\partial^2 \bar{\Psi}}{\partial x_1^2}\Big|_{x_1=0} + \text{----}$$

$$= \sqrt{\nu_\infty LU}\left[\frac{a}{2}\zeta_o^2 - \frac{a^2}{2.5!}\zeta_o^5 + \frac{11}{4}\frac{a^3}{8!}\zeta_o^8 \text{----}\right]$$

$$+ \frac{x_1}{L}\sqrt{\nu_\infty UL}\left[-\frac{a}{4}\zeta_o^2 + \frac{a^2}{5!}\zeta_o^5 - \frac{77a^3}{8.8!}\zeta_o^8 \text{----}\right]$$

$$+ \frac{x_1^2}{L^2}\sqrt{\nu_\infty LU}\left[\frac{3a}{8}\zeta_o^2 - \frac{14}{5!8}a^2\zeta_o^5 + \frac{11.47}{16.8!}a^3\zeta_o^8\right] + \text{---}.$$

Since $\zeta_o = y$

$$\bar{\Psi}_o = \frac{\bar{\Psi}}{\sqrt{\nu_\infty LU}} = \frac{a}{2}y^2 - \frac{a^2}{2.5!}y^5 + \frac{11}{4}\frac{a^3}{8!}y^8 \text{----}$$

$$+ x\left(-\frac{a}{4}y^2 + \frac{a^2}{5!}y^5 - \frac{77}{8.8!}a^3 y^8 \text{----}\right)$$

$$+ \frac{x^2}{2!}\left(\frac{3}{8}a y^2 - \frac{14}{8.5!}a^2 y^5 + \frac{11.47}{16.8!}a^3 y^8 \text{---}\right)$$

Now in terms of the inner variables, $y = \xi\eta$, so

$$\psi_o = \frac{a}{2}\,\xi^2\eta^2 - \frac{a^2}{2.5!}\,\xi^5\eta^5 + \frac{11}{4}\,\frac{a^3}{8!}\,\xi^8\eta^8$$

$$+ \xi^n\left(-\frac{a}{4}\,\xi^2\eta^2 + \frac{a^2}{5!}\,\xi^5\eta^5 - \frac{77}{8.8!}\,a^3\xi^8\eta^8 + \cdots\right)$$

$$+ \frac{\xi^{2n}}{2!}\left(\frac{3a}{8}\,\xi^2\eta^2 - \frac{14}{8.5!}\,a^2\xi^5\eta^5 + \frac{11.47}{16.8!}\,a^3\xi^8\eta^8 + \cdots\right)$$

From (11) the inner stream function is

$$\psi_i = \xi^m f(\xi,\eta) = \xi^m\left[f_o(\eta) + \xi f_1(\eta) + \xi^2 f_2(\eta) + \xi^3 f_3(\eta) + \cdots\right]$$

By matching

$$\psi_{\substack{\text{inner}\\ \eta\to\infty}} \quad \rightarrow \quad \psi_{\substack{\text{outer}\\ y\to 0}}$$

We obtain $\quad m = 2 \quad$ $\quad n = 3$

and

$$\left.\begin{aligned}
f_o(\eta) &\sim \frac{a}{2}\,\eta^2\\
f_1(\eta) &= 0\\
f_2(\eta) &= 0\\
f_3(\eta) &\sim -\frac{a^2}{2.5!}\,\eta^5 - \frac{a}{4}\,\eta^2\\
f_4(\eta) &= 0\\
f_5(\eta) &= 0\\
f_6(\eta) &\sim \frac{11}{4}\,\frac{a^3}{8!}\,\eta^8 + \frac{a^2}{5!}\,\eta^5 + \frac{3a}{2.8}\,\eta^2
\end{aligned}\right\} \quad \text{as } \eta\to\infty$$

Similarly by matching $\quad u_{\substack{\text{inner}\\ \eta\to\infty}} \quad \rightarrow \quad u_{\substack{\text{outer}\\ y\to 0}}$

one has

$$\left.\begin{aligned} f_o'(\eta) &\sim a\eta \\ f_1'(\eta) &= 0 \\ f_2'(\eta) &= 0 \\ f_3'(\eta) &\sim -\frac{a^2}{2.4!}\eta^4 - \frac{a}{2}\eta \\ f_4'(\eta) &= 0 \\ f_5'(\eta) &= 0 \\ f_6'(\eta) &\sim \frac{11}{4}\frac{a^3}{7!}\eta^7 + \frac{a^2}{4!}\eta^4 + \frac{3a}{8}\eta \end{aligned}\right\} \quad \text{as } \eta \to \infty$$

Thus we can rewrite Eq. (14) as follows

$$3 f_o''' + 2 f_o f_o'' - f_o' = 0$$

$$\left.\begin{aligned} f_o &\sim \frac{a}{2}\eta^2 \\ f_o' &\sim a\eta \end{aligned}\right\} \quad \eta \to \infty \qquad (15)$$

$$f_o' = 0 \qquad \eta \to -\infty$$

$$3 f_3''' + 2 f_o f_3'' - 5 f_o' f_3' + 5 f_o'' f_3 = 0$$

$$\left.\begin{aligned} f_3(\eta) &\sim -\frac{a^2}{2.5!}\eta^5 - \frac{a}{4}\eta^2 \\ f_3'(\eta) &\sim \frac{a^2}{2.4!}\eta^4 - \frac{a}{2}\eta \end{aligned}\right\} \quad \text{as } \eta \to \infty \qquad (16)$$

$$f_3'(\eta) = 0 \qquad \eta \to -\infty$$

$$3 f_6''' + 2 f_o f_6'' - 8 f_o' f_6' + 8 f_o'' f_6 = 4(f_3')^2 - 5 f_3 f_3''$$

$$\left.\begin{aligned} f_6(\eta) &\sim \frac{11}{4}\frac{a^3}{8!}\eta^8 + \frac{a^2}{5!}\eta^5 + \frac{3a}{16}\eta^2 \\ f_6'(\eta) &\sim \frac{11}{4}\frac{a^3}{7!}\eta^7 + \frac{a^2}{4!}\eta^4 + \frac{3a}{8}\eta \end{aligned}\right\} \quad \text{as } \eta \to \infty \qquad (17)$$

$$f_6'(\eta) = 0 \qquad \eta \to -\infty \quad ,$$

and $f_1 \equiv f_2 \equiv f_4 \equiv f_5 \equiv 0$ (Appendix A)

The first two differential equations for f_o and f_3 were solved numerically, and the results are tabulated and plotted in Figures (4A)-(4D). A special numerical method for solving the nonlinear third order differential equation for f_o is introduced in the Appendix.

The variation of the velocity component in the y direction in the shear layer can be obtained by differentiating the stream function with respect to x, that is, in the outer layer for small y

$$v = -\frac{\partial \psi}{\partial x} = \tfrac{1}{2}\left[\frac{a}{2} y^2 - \frac{2a^2}{5!} y_5 + \frac{77}{4.8!} a^3 y^8 + \cdots\right]$$

$$- \tfrac{1}{4} x\left[\frac{3}{2} a y^2 - \frac{3}{5!} a^2 y^5 + \frac{99}{4.8!} a^3 y^8 + \cdots\right]$$

In terms of the inner variable

$$v = + \frac{a}{4} \xi^2 \eta^2 - \frac{a^2}{5!} \xi^5 \eta^5 + \frac{77}{8.8!} \xi^8 \eta^8 -- + \cdots$$

$$- \tfrac{1}{4}\left[\frac{3}{2} a \xi^5 \eta^2 - \frac{3}{5!} a^2 \xi^8 \eta^5 + \cdots\right] + \cdots$$

In the inner layer

$$v = -\frac{\partial}{\partial x}[\xi^2 f(\xi, \eta)]$$

$$= \frac{1}{3}[(\eta f_o' - 2 f_o)\xi^{-1}$$

$$+ \xi^2(\eta f_3' - 5 f_3) + \text{----} + \xi^5(\eta f_6' - 8 f_6)] + \cdots$$

By substituting the asymptotic values of f_o', f_o, f_1', f_1 ---- as $\eta \to \infty$ into the above equation, or by utilizing the relations

$$\left.\begin{aligned} \eta f_o' - 2 f_o &= 0 \\ \eta f_3' - 5 f_3 &= \frac{3}{4} a \eta^2 \\ \eta f_6' - 8 f_6 &= -3\left[\frac{a^2}{5!} \eta^5 + \frac{3}{8} \eta^2\right] \end{aligned}\right\} \quad \eta \to \infty$$

one can see that

$$v_{\text{inner}} \underset{\eta \to \infty}{\to} v_{\text{outer}} \quad y \to \infty$$

This result implies that no additional displacement in the y direction at the outer edge of the shear layer will be induced because of the presence of the mixing layer. Also it is consistent with the assumption made at the beginning that the static pressure p is constant to the first order throughout the shear layer.

The solution of the energy equation can be obtained easily by the following relation

$$H = A + Bu$$

Boundary conditions for the enthalpy distribution are as follows:

(i) For a "cold" wall

For $x < 0$ $\quad H = 1 \quad$ as $y_1 \to \infty$

$$H = \frac{H_w}{H_\infty} \qquad y_1 = 0$$

For $x > 0$ $\quad H = 1 \quad$ as $y_1 \to \infty$

$$H = \frac{H_b}{H_\infty} \qquad y_1 \to -\infty$$

It is reasonable to assume $H_w = H_b$.

Thus

$$A = \frac{H_w}{H_\infty}$$

$$B = 1 - A = \frac{H_\infty - H_w}{H_\infty}$$

Then

$$H = \frac{1}{H_\infty} [H_w + (H_\infty - H_w)u] \tag{18}$$

or

$$\frac{T}{T_\infty} = \frac{T_w}{T_\infty} + \left[1 - \frac{T_w}{T_\infty} + \frac{\gamma-1}{2} M_\infty^2\right]u - \frac{\gamma-1}{2} M_\infty^2 u^2$$

(ii) For an adiabatic wall

$H \equiv 1$ is the solution where $H_w = H_c = H_\infty$, and

$$\frac{T}{T_\infty} = 1 + \frac{\gamma-1}{2} M_\infty^2 (1-u^2)$$

Finally the stream function and x-component of velocity in the mixing region are given by the expressions

$$\psi(x, y) = x^{\frac{2}{3}}\left[f_o(\eta) + x f_3(\eta) + x^2 f_6(\eta) + \text{---}\right]$$

and

$$u(x, y) = x^{\frac{1}{3}}\left[f_o'(\eta) + x f_3'(\eta) + x^2 f_6'(\eta) + \text{---}\right]$$

where $\eta = y/x^{\frac{1}{3}}$

Since $f_o(\eta)$ vanishes at $\eta \cong 0.9$ (Fig. 4A) the dividing streamline lies above the x_1-axis and has the shape $y = \text{const.}\ x^{\frac{1}{3}}$ initially. This result agrees with the result of Rott and Hakkinen[8]. The shape of the dividing streamline in the next approximation is found from the relation $x = -\frac{f_o(\eta)}{f_3(\eta)}$; $\eta_{\psi=0}$ increases slightly with increasing x. The value of $u = u^*$ along the dividing streamline can then be found, and is plotted in Fig. 6 up to $x = 0.5$, the joining point with the far-field (Section IV). The growth of the mixing layer and some typical velocity profiles are shown in Fig. 7.

(2) Arbitrary Initial Velocity Profile With a Finite Slip

In this case the initial velocity profile has a finite slip on the dividing streamline. Instead of using free stream velocity as reference

velocity we choose the slip velocity u_{1_s} to non-dimensionalize the velocity field.

Then

$$u = \frac{u_1}{u_{1_s}} \qquad \psi_s = \frac{\psi}{\sqrt{u_{1_s} L \nu_\infty}}$$

$$v = \frac{\bar{v}}{u_{1_s}} \sqrt{R_s} \qquad R_s = \frac{u_{1_s} L}{\nu_\infty}$$

$$x = \frac{X-L}{L} \qquad H = \frac{S}{H_\infty}$$

$$y = \frac{Y}{L} \sqrt{R_s}$$

The normalized stream function for the inner sub-layer is

$$\psi_s(x, y) = \xi^m f(\xi, \eta)$$

where

$$\xi = x^{1/n} \qquad \eta = \frac{y}{\xi} .$$

The matching procedure is similar to that of case 1, but the inner series expansion is assumed to be of the following form for convenience later:

$$f(\xi, \eta) = f_0(\eta) + a\xi f_1(\eta) + b\xi^2 f_2(\eta) \tag{19}$$

In order to calculate the subsequent development of the "outer" viscous flow, not only $u_{outer}(o, y)$ must be specified, but also $v(o, y)$, and all the partial derivatives $\frac{\partial^k v}{\partial x^k}(o, y)$. By referring to Eq. (8) and (9) one sees that these equations reduce to a single first-order linear differential equation for $v(o, y)$ when $u(o, y)$ is specified. Therefore the value of $v(o, y)$ at only <u>one</u> location $y = y^*$ is sufficient to determine the initial v-distribution and also $\frac{\partial u}{\partial x}(o, y)$ [Eq. (8)]. Similarly, by differentiating Eq. (8) and (9) s-times with respect to x one can easily show that the resulting equations reduce to a first-order linear differential equation

for $\left(\frac{\partial^s v}{\partial x^s}\right)_{x=0}$, so the value of $\frac{\partial^s v}{\partial x^s}(o, y)$ at only one point is required to determine $\frac{\partial^{s+1} u}{\partial x^{(s+1)}}(o, y)$ uniquely.

As an illustrative example, suppose we consider the special, simple case in which $u(o, y) \neq 0$, but $v(0, 0) = \left(\frac{\partial v}{\partial x}\right)_{o, o} = \left(\frac{\partial^s v}{\partial x^s}\right)_{o, o} = 0$, all s. The calculation is carried out most conveniently by substituting an expansion of the form

$$\psi_{s_{outer}}(x, y) = \varphi_{s_o}(y) + x\varphi_{s_1}(y) + \frac{x^2}{2!}\varphi_{s_2}(y) + \frac{x^3}{3!}\varphi_{s_3}(y) + \cdots$$

$$u_{outer}(x, y) = \varphi_{s_o}'(y) + x\varphi_{s_1}'(y) + \frac{x^2}{2!}\varphi_{s_2}'(y) + \frac{x^3}{3!}\varphi_{s_3}'(y) + \cdots \quad (20)$$

$$v_{outer}(x, y) = -\left[\varphi_{s_1}(y) + x\varphi_{s_2}(y) + \frac{x^2}{2!}\varphi_{s_3}(y) + \cdots\right]$$

into the boundary layer equations. By collecting terms of order x^r, where $r = 0, 1, 2 \cdots$, and equating the sum of the coefficients of x^r to zero, one obtains the following equations for φ_{s_1}, φ_{s_2}, φ_{s_3} $\cdots$.

$$\varphi_{s_o}''' - \varphi_{s_o}'\varphi_{s_1}' + \varphi_{s_1}\varphi_{s_o}'' = 0$$

$$\varphi_{s_1}''' - \varphi_{s_1}'^2 - \varphi_{s_o}'\varphi_{s_2}' + \varphi_{s_1}\varphi_{s_1}'' + \varphi_{s_2}\varphi_{s_o}'' = 0 \quad (21)$$

$$\varphi_{s_2}''' - \varphi_{s_o}'\varphi_{s_3}' - 3\varphi_{s_1}\varphi_{s_2}' + \varphi_{s_1}\varphi_{s_2}'' + 2\varphi_{s_2}\varphi_{s_1}'' + \varphi_{s_3}\varphi_{s_o}'' = 0$$

Since $u = \varphi_{s_o}'(y) \to \frac{u_\infty}{u_{1_s}}$ as $y \to \infty$, we must have $\varphi_{s_1}' = \varphi_{s_2}'(y) = \cdots \to 0$ as $y \to \infty$. Inspection of Eq. (21) shows that this condition is automatically satisfied if φ_{s_o}'', φ_{s_o}''', etc. $\to 0$ sufficiently fast as $y \to \infty$. However the condition that $v(o, o)$ and all partial x-derivatives of v vanish at $x = 0$, $y = 0$ means that [Eq. (20)] $\varphi_{s_1}(0) = \varphi_{s_2}(0) = \cdots = 0$. By employing these boundary conditions Eq. (21) are solved by quadrature:

$$\varphi_{s_1}(y) = \varphi_{s_o}' \int_o^y \frac{\varphi_{s_o}'''(y')}{\varphi_{s_o}'^2(y')}\, dy'$$

$$\varphi_{s_2}(y) = \varphi_{s_o}' \left[\int_o^y \frac{\varphi_{s_1}\varphi_{s_1}''}{\varphi_{s_o}'^2}\, dy' + \int_o^y \frac{\varphi_{s_1}'''}{\varphi_{s_o}'^2}\, dy' - \int_o^y \frac{\varphi_{s_1}'^2}{\varphi_{s_o}'^2}\, dy' \right],$$

etc.

[Note that $\varphi_{s_1}(\infty)$, $\varphi_{s_2}(\infty)$, etc. are all $\neq 0$]

Suppose that the initial velocity profile with slip U_{1s} at $y = 0$ is assumed to be of the following form as $y \to 0$:

$$u_o(y) = \varphi_{s_o}'(y) = 1 + Ay + By^2 + Cy^3 + Dy^4 + \text{---}$$

where A, B, C and D are constant coefficients describing the shape of the initial velocity profile. As $y \to 0$ (Eq. 21a)

$$\varphi_{s_1}(y) \to 2By + 3Cy^2 + y^3 (4D\text{-}AC + \tfrac{2}{3} B^2) + \text{---}$$

$$\varphi_{s_2}(y) \to 6(4D\text{-}AC)y + \text{---}$$

By substituting these expressions into Eq. (20) one has

$$\left[\psi_s(x, y)_{\text{outer}}\right]_{y \to 0} = \varphi_{s_o}(y) + x\,\varphi_{s_1}(y) + \frac{x^2}{2!}\varphi_{s_2}(y) + \text{----}$$

$$= y + \frac{A}{2} y^2 + \frac{B}{3} y^3 + \frac{C}{4} y^4 + \frac{D}{5} y^5 + \text{----}$$

$$+ x \left[2By + 3Cy^2 + (4D - AC + \tfrac{2}{3} B^2)y^3 + \text{---}\right]$$

$$+ \frac{x^2}{2!}\left[6\,(4D - AC)y + \text{----}\right] + \text{---}$$

By changing to inner variables ($y = \xi\eta$, $x = \xi^n$), we obtain

$$[\psi_s(\xi,\eta)] = \xi\eta + \frac{A}{2}\xi^2\eta^2 + \frac{B}{3}\xi^3\eta^3 + \frac{C}{4}\xi^4\eta^4 + \frac{D}{5}\xi^5\eta^5 + \cdots$$

$$+ \xi^n[2B\xi\eta + 3C\xi^2\eta^2 + (4D - AC + \tfrac{2}{3}B^2)\xi^3\eta^3 + \cdots]$$

$$+ \frac{\xi^{2n}}{2!}[6(4D - AC)\xi\eta + \cdots] + \cdots$$

The inner expansion is

$$\psi_s(\xi,\eta) = \xi^m f_o(\eta) + a\,\xi^{m+1} f_1(\eta) + b\,\xi^{m+2} f_2(\eta) + \cdots$$

where $n = m+1$.

By matching $\psi_{\substack{\text{inner}\\ \eta\to\infty}} \to \psi_{\substack{\text{outer}\\ y\to 0}}$ we get $m = 1$ and $n = m+1 = 2$.

Thus

$$\psi_s(\xi,\eta) = \xi f_o(\eta) + a\,\xi^2 f_1(\eta) + b\,\xi^3 f_2(\eta) + \cdots \qquad (22)$$

where $a = A$, $b = B$

and $f_o(\eta) \sim \eta$

$f_1(\eta) \sim \frac{1}{2}\eta^2$ as $\eta \to \infty$

$f_2(\eta) \sim \frac{1}{3}\eta^3 + 2\eta$

Similarly by matching u_{inner} and u_{outer} we obtain

$f_o'(\eta) \sim 1$

$f_1'(\eta) \sim \eta$ as $\eta \to \infty$

$f_2'(\eta) \sim \eta^2 + 2$

After substituting $[\psi_s(\xi,\eta)]_{\text{inner}}$ into the momentum equation and collecting terms of order ξ^m we obtain three sets of differential equations, with the corresponding boundary conditions:

$$2 f_o''' + f_o f_o'' = 0$$

$$\left.\begin{aligned} f_o &\sim \eta \\ f_o' &\sim 1 \end{aligned}\right\} \quad \eta \to \infty$$

$$f_o' \sim 0 \qquad \eta \to -\infty$$

$$2 f_1''' + f_o f_1'' - f_o' f_1' + 2 f_o'' f_1 = 0$$

$$\left.\begin{aligned} f_1 &\sim \tfrac{1}{2}\eta^2 \\ f_1' &\sim \eta \end{aligned}\right\} \eta \to \infty$$

$$f_1' = 0 \qquad \eta \to -\infty$$

$$2 f_2''' + f_o f_2'' - 2 f_o' f_2' + 3 f_o'' f_2 = -2 f_1 f_1'' + (f')^2$$

$$\left.\begin{aligned} f_2 &\sim \tfrac{1}{3}\eta^3 + 2\eta \\ f_2' &\sim \eta^2 + 2 \end{aligned}\right\} \quad \eta \to \infty$$

$$f_2' = 0 \qquad \eta \to -\infty$$

The final formula for the velocity profile in the mixing region is given by

$$u = f_o'(\eta) + A\, x^{\frac{1}{2}} f_1'(\eta) + B\, x\, f_2'(\eta) + 0(x^{\frac{3}{2}}) \tag{23}$$

while

$$\psi_{\text{inner}} = x^{\frac{1}{2}} f_o(\eta) + A\, x\, f_1(\eta) + B x^{\frac{3}{2}} f_2(\eta) + \text{---}$$

The velocity profile depends not only on these universal functions f_o, f_1, f_2 and so on, but also on the parameters A, B, --- of the initial profile. A tabulation of the universal functions is given at the end of this paper and these functions are plotted in Figs. (5A) through (5H). The progress of u^* with x/L is shown in Fig. 6 for quadratic initial profiles, where the triangles indicate the junctions with the far field solution (Sec. IV).

The solution for the enthalpy field is similar to the case of the initial Blasius profile.

Now the y-component of the velocity in the inner sublayer must match the corresponding velocity component in the outer layer.

$$v = -\frac{\partial \psi_s}{\partial x} = -\varphi_{s_1}(y) - x\,\varphi_{s_2}(y) + \cdots \quad , \quad \text{or}$$

$$v = -[2By + 3Cy^2 + \cdots] - x[6(4D - AC)y + \cdots] + \cdots$$

In terms of inner layer variables,

$$v = -2B\xi\eta - 3C\xi^2\eta^2$$

In the inner layer

$$v = -\frac{\partial \psi}{\partial x} = -\frac{\partial}{\partial x}[x^{\frac{1}{2}} f(\xi, \eta)] = -\frac{1}{2\xi}(f + \xi f_\xi - \eta f_\eta)$$

$$= \frac{1}{2\xi}[\{\eta f_o'(\eta) - f_o\} + A\{\eta f_1'(\eta) - 2f_1(\eta)\}\xi + B(\eta f_2' - 3f_2)\xi^2 + \cdots]$$

Since

$$\left.\begin{aligned} &\eta f_o'(\eta) - f_o = 0 \\ &\eta f_1'(\eta) - 2f_1(\eta) = 0 \\ &\eta f_2' - 3f_2 = -4\eta \end{aligned}\right\} \quad \text{as } \eta \to 0$$

$$v \to -2B\xi\eta + \cdots \qquad \text{as } \eta \to \infty$$

so that

$$v_{\text{inner}} \to v_{\text{outer}}$$

$$\eta \to \infty \qquad y \to o$$

This result tells us that in the slip case there is no <u>additional</u> lateral displacement produced by the mixing process.

As $x \to 0$, $u \to f_o'(\eta)$ and $\psi_{inner} \to x^{\frac{1}{2}} f_o(\eta)$, according to Eq. (23). Now the differential equation for f_o is identical with the corresponding equation for Chapman's problem, but the boundary conditions on $f_o(\eta)$ are slightly different. Because of our insistence that the additional induced normal velocity component should vanish in the outer layer, the Chapman condition $f_o(0) = 0$ is replaced by the condition $f_o \to \eta$ as $\eta \to \infty$. By referring to Fig. 5A, one can see that in the present solution f_o vanishes when $\eta = -0.5273$, and Fig. 5B shows that $f_o' = 0.587$ along this parabola. In other words the dividing streamline lies below the x-axis at first when the initial slip velocity is not zero (Fig. 8), but the velocity normalized by the slip velocity is the same function of $\psi/\sqrt{x}$ as in Chapman's solution. On the x_1-axis itself $u \to 0.68$ and $\psi/\sqrt{x} \to 0.3$ as $x \to 0$.

According to Table II, $f_0(0) = 0.3378$ and $f_1(0) = 0.8457$, so $\psi(x, 0) = 0.3x^{\frac{1}{2}} - 0.84Ax + \text{---}$, and the dividing streamline crosses the x_1-axis again when $x = x_o \cong \frac{0.13}{A^2}$. For example, for an initial quadratic profile with $u_{1_s} = 0.4$, $A \cong 0.6$, so $x_o \cong 0.38$ (Fig. 8). This behavior of the dividing streamline can be understood on the basis of simple physical considerations. When the initial profile has a finite slip velocity the x-component of velocity drops instantaneously to a value of $0.68\, u_{1_s}$ along the x_1-axis. As the mixing region grows with increasing x_1 the mass flux defect contributed by the mixing increases at first (Fig. 8), so the contribution to the displacement thickness is initially positive and increasing. Thus the dividing streamline must have a negative slope and must lie below the x_1-axis initially in order to counterbalance the normal velocity component induced by the mixing

region. However, the velocity on the x_1-axis increases with downstream distance $[u(x, 0) \rightarrow 0.69 + 0.58\ Ax^{\frac{1}{2}} + 1.03\ Bx] + \cdots$. For small initial slip velocity u(x,0) soon reaches and then exceeds u_{1_s} (Fig. 6), and the mass flux defect in the mixing region changes to a mass flux surplus. Thus the slope of the dividing streamline must change sign from negative to positive, and the dividing streamline must cross the x_1-axis and lie above it in order not to disturb the streamlines in the outer shear layer. The smaller the value of u_{1_s} the sooner the dividing streamline crosses the x_1-axis.

Now one knows that u(x, 0) will not exceed the final asymptotic value of 0.573U in any event, so when the initial slip velocity is large enough ($u_{1_s} > 0.573U$, roughly) then $u(x, 0) > u_{1_s}$ and the dividing streamline always lies <u>below</u> the x_1-axis in the near field.

On the other hand when the initial velocity profile is a no-slip profile the velocity along the x_1-axis begins to increase immediately after the flow leaves the edge. The contribution to the displacement thickness made by the mixing region is negative, and its magnitude increases with increasing x_1. One concludes that the dividing streamline must have a <u>positive slope</u> in this case, and must lie <u>above</u> the x_1-axis in the near field, as shown in Fig. 7.

IV. FAR FIELD SOLUTION: MOMENTUM INTEGRAL METHOD

The momentum integral method is a very useful and convenient approximate method for treating boundary layer and separated flow problems. For the constant pressure mixing problem, Kubota and Dewey[4] applied the integral method in a direct and simple manner. They represented the velocity profile by a simple analytic function containing several parameters that are allowed to vary with x. They divided the shear layer into two portions above and below the dividing streamline. By multiplying the momentum equation by $u^j (j = 0, 1, 2, 3--)$ and integrating across the shear layer, coupled ordinary differential equations are obtained which describe the variation of the velocity profile parameters in the x-direction. Boundary conditions are also applied at the extremities of the shear layer. The total number of boundary conditions and moment equations must be equal to the number of parameters appearing in the velocity profile. Kubota and Dewey integrated the differential equations numerically, starting with an assumed velocity profile at $x = 0$. The calculation is continued until a similar profile corresponding to $x \to \infty$ is reached.

In the present problem the velocity profile changes rapidly with distance in the x-direction just after the flow leaves the edge. Thus the momentum integral method is not expected to give good results in the near-field. But after a certain distance the velocity profile changes slowly and the momentum integral method should be applicable. Integration of the equations is started from some $x > 0$ where the new initial profile is determined by the near-field solution.

The shear layer is divided into two layers: region (A), $\delta_1 > y > 0$ and region (B), $-\delta_2 < y < 0$. Now integrate equation (9) separately in the two regions

$$\int_o^{\delta_1} u \frac{\partial u}{\partial x} dy + \int_o^{\delta_1} v \frac{\partial u}{\partial y} dy = \int_o^{\delta_1} \frac{\partial^2 u}{\partial y^2} dy$$

and

$$\int_{-\delta_2}^{o} u \frac{\partial u}{\partial x} dy + \int_{-\delta_2}^{o} v \frac{\partial u}{\partial y} dy = \int_{-\delta_2}^{o} \frac{\partial^2 u}{\partial y^2} dy$$

where v can be replaced by $v = -\int_o^y (\frac{\partial u}{\partial x})\, dy$. Upon integration the above two equations can be written as

$$\frac{d}{dx}\left[\delta_1 \int_o^1 f(1-f)\, d\eta\right] = \frac{1}{\delta_1} \left(\frac{\partial f}{\partial \eta}\right)_{\eta=0} \tag{23a}$$

and

$$\frac{d}{dx}\left[\delta_2 \int_1^o g^2\, d\xi\right] = \frac{1}{\delta_2} \left(\frac{\partial g}{\partial \xi}\right)_{\xi=0} \tag{23b}$$

where

$f(\eta) = u$ $\qquad \eta = \frac{y}{\delta_1}$ $\qquad$ for $y > 0$

$g(\eta) = u$ $\qquad \xi = \frac{y}{\delta_2}$ $\qquad$ for $y < 0$

We take the velocity profiles in the two layers to be of the following simple forms:

$$\begin{aligned} f(\eta) &= 1 - (1-u^*)(1-\eta)^n \\ g(\xi) &= u^*(\xi+1)^r \end{aligned} \qquad n, r \geq 1 \tag{24}$$

where u^* is the normalized velocity along the dividing streamline, and n and r are arbitrary constants.

The shear stress must be continuous at y = 0, so

$$\left(\frac{\partial f}{\partial \eta}\right)_{\eta=0} = \frac{\delta_1}{\delta_2}\left(\frac{\partial g}{\partial \xi}\right)_{\xi=0} \tag{25}$$

From equations (24) and (25)

$$\frac{\delta_2}{\delta_1} = \frac{r\,u^*}{n(1-u^*)} \tag{26}$$

and Eqs. (23a) and (23b) become

$$\frac{d}{dx}\left[\delta_1(1-u^*)\left(\frac{1}{n+1} - \frac{1-u^*}{2n+1}\right)\right] = \frac{n(1-u^*)}{\delta_1} \tag{27}$$

$$\frac{d}{dx}\left[\delta_2 \frac{u^{*2}}{(2\gamma+1)}\right] = -\frac{r\,u^*}{\delta_2} \tag{28}$$

Three unknowns δ_1, δ_2 and u^* are determined by the above three equations and the corresponding initial conditions.

$$\delta_1 \to \delta_{10} \qquad \delta_2 \to \delta_{20} \qquad u^* \to u_o^* \qquad \text{as } x = x_o \quad ,$$

where n and r are determined by the shape of the initial velocity profiles. Kubota and Dewey used n = r = 2 and Reeves used n = r = integers > 1. In the present problem n and r may be any positive numbers greater than unity.

A relation between δ_1 and u^* can easily be obtained by direct integration of Eq. (27), namely

$$\frac{\delta_1}{\delta_{10}} = \frac{(1-u_o^*)\left(\frac{1}{n+1} - \frac{1-u_o^*}{2n+1}\right) - \frac{r\,u_o^{*3}}{n(1-u_o^*)(2r+1)}}{(1-u^*)\left(\frac{1}{n+1} - \frac{1-u^*}{2n+1}\right) - \frac{r\,u^{*3}}{n(1-u^*)(2r+1)}} \tag{29}$$

From equation (29) if we let $\delta_1/\delta_{10} \to \infty$, the limiting case of Chapman's similarity solution should be reached. Hence

$$(n+1)(n-r)u^{*3} - n(2r+1)(n+2)u^{*2} - n(2r+1)(n-1)u^* + n^2(2r+1) = 0$$

The far field region for the Blasius initial profile was solved by using the above method starting from $x = 0.5$. It is found that $n = 1.5$ and $r = 2.7$ in order to fit the velocity profile at $x = 0.5$. In this particular case $u^* = 0.579$ as $x \to \infty$, which is very close to Chapman's value of 0.587.

For a particular slip case with $\frac{u_{10}}{U} = 0.4$ the numerical integration is started from $x = 0.5$. Here n and r are found to be 2.4 and 2.5 respectively, and $u^* = 0.594$ as $x \to \infty$.

The growth of u^* in the far field is shown in Fig. 6. The results for the slip case are in good agreement with Kubota and Dewey's quadratic integral solution and Reeves' high shear integral solution. The Blasius case almost identically coincides with Denison and Baum's solution for Blasius initial velocity profile. Since the velocity along the dividing streamline is larger for the finite slip case than for the non-slip initial profile, the vorticity is larger and u^* increases much faster with x (Fig. 6).

Although the momentum integral method gives good results for u^* and shear layer thickness it is not expected to furnish highly accurate velocity profiles. For this reason no attempt has been made here to match the y-component of velocity and the location of the dividing streamline with the near field solution at the junction point. By including interaction with an "external" supersonic flow (for example) one could determine the correct shear layer flow approaching the Chapman solution as an asymptotic limit as $x \to \infty$, either by using an integral method or by using a finite-difference approach.

V. SUMMARY AND CONCLUSIONS

1. The present theoretical study shows that the constant-pressure laminar mixing of an initial shear layer with a quiescent fluid occurs without developing a line of singularities at the starting position ($x = 0$). The only singularity lies at the origin $x = 0_1$, $y = 0$ itself. The line of singularities is removed by abandoning the conventional restriction that the dividing streamline must coincide with the x-axis.

2. For an initial Blasius velocity profile with no slip the progress of the inner mixing layer in the near-field is described by the stream function $\psi(x, y) = x^{\frac{2}{3}} [f_o(\eta) + x f_3(\eta) + x^2 f_6(\eta) + \text{---}]$ where $\eta = y/(x^{\frac{1}{3}})$ and the functions f_o, f_3 are given in Figures 4A-4D, and Table I.

For an arbitrary initial velocity profile with finite slip of the form $\frac{u_1}{u_{1_s}} = 1 + Ay + By^2 + Cy^3 + \text{---}$ as $y \to 0$, the inner mixing layer in the near-field is described by the stream function

$$\psi(x, y) = x^{\frac{1}{2}} f_o(\eta) + Ax f_1(\eta) + Bx^{\frac{3}{2}} f_2(\eta) + \text{---}$$

where f_o, f_1, f_2 are given in Figures 5A-5H, and Table II.

3. For the Blasius initial velocity profile the dividing streamline lies above the x-axis in the near field. For the arbitrary initial velocity profile with finite slip the dividing streamline always lies below the x-axis at first. When the slip velocity < 0.573 U (approx.) the dividing streamline later crosses the x-axis at some location and lies above this axis; the crossing point is closer to the origin the smaller the initial slip velocity. When the slip velocity > 0.573 U the dividing streamline stays below the x-axis in the near-field. This behavior

is quite plausible on the basis of simple mass flux considerations.

4. The far-field development is obtained by using a momentum integral method starting at an appropriate downstream location, where the velocity on the dividing streamline and the shear layer thickness are joined to the new field solution. In this manner the progress of the mixing over the whole field can be followed in any particular problem for an arbitrary initial velocity profile.

5. All of these results are readily transformed to a compressible flow by using the Stewartson transformation.

REFERENCES

1. Lees, L. and Hromas, L.: "Turbulent Diffusion in the Wake of a Blunt-Nosed Body at Hypersonic Speeds," J. A. S. 29:8, 976-993 (1962).

2. Charters, A. C. and Thomas, R. N.: "The Aerodynamic Performance of Small Spheres from Subsonic to High Supersonic Velocities," J. A. S., 12, 468-476 (1945).

3. Chapman, D. R.: "Laminar Mixing in a Compressible Fluid," NACA Tr No. 958 (1950).

4. Kubota, T. and Dewey, C. F.: "Momentum Integral Methods for the Laminar Free Shear Layer," AIAA J. 2, 625-629 (1964).

5. Reeves, B. L.: "Constant Pressure Laminar Mixing with 'Arbitrary' Initial Velocity and Stagnation Enthalpy Profiles," Grad. Aero. Lab., Calif. Inst. of Tech., Separated Flows Research Project, Internal Memo 2, March 1964.

6. Denison, M. R. and Baum, E.: "Compressible Free Shear Layer with Finite Initial Thickness," AIAA J. 1, 342-349 (1963).

7. Toba, K.: "Analysis of Free Shear Layer with Finite Initial Thickness and its Application to Base Flow," Douglas Report SM-45943, 14 May 1964.

8. Rott, N. and Hakkinen, R. J.: "Numerical Solutions for Merging Shear Flows," Douglas Report SM-47809, Feb. 1965.

9. Goldstein, S.: "Concerning Some Solutions of the Boundary Layer Equations in Hydrodynamics," Proceedings of the Cambridge Philosophical Society, Vol. 26, pp. 1-30 (1930).

APPENDIX A

The differential equation for f_1 and its boundary conditions are:

$$3 f_1''' + 2 f_o f_1'' - 3 f_o' f_1' + 3 f_o'' f_1 = 0$$

$$f_1(\eta) = 0 \qquad \eta \to \infty$$

$$f_1'(\eta) = 0 \qquad \eta \to \infty$$

$$f_1'(\eta) = 0 \qquad \eta \to -\infty$$

Since the above differential equation is linear and homogeneous, we can write the general solution in terms of three linearly independent solutions

$$f_1(\eta) = A\, g(\eta) + B\, h(\eta) + C\, p(\eta) \tag{A1}$$

Now match $\left(\frac{\partial u}{\partial y}\right)_{\text{inner}}$ with $\left(\frac{\partial u}{\partial y}\right)_{\text{outer}}$

$$\left.\frac{\partial u}{\partial y}\right)_{\text{outer}} = \frac{\partial^2 \psi}{\partial y^2} = a - \frac{a^2}{2.3!}\, y^3 + \frac{11}{4}\,\frac{a^3}{6!}\, y^6 \text{ --- } + x\left[\frac{a}{2} - \frac{5}{2}\,\frac{a^2}{4!}\, y^3 + \text{ --- }\right]$$

$$+ \frac{x^2}{2!}\left[- \frac{11}{4}\, a + \text{ --- }\right]$$

$$= a - \frac{a^2}{2.3!}\, \xi^3 \eta^3 + \frac{11}{4}\,\frac{a^3}{6!}\, \xi^6 \eta^6 \text{ ---- } + \xi^3\left[\frac{a}{2} - \frac{5}{2}\,\frac{a^2}{4!}\, \xi^3 \eta^3 + \text{--}\right]$$

$$+ \frac{\xi^6}{2!}\left[- \frac{11}{4}\, a + \text{ --- }\right]$$

$$\left.\frac{\partial u}{\partial y}\right)_{\text{inner}} = f_{\eta\eta} = f_o''(\eta) + \xi\, f_1''(\eta) + \xi f_1''(\eta) + \xi^3 f_2''(\eta) + \text{ --- }$$

by matching

$$\left.\frac{\partial u}{\partial y}\right)_{\substack{\text{inner} \\ \eta \to \infty}} = \left.\frac{\partial u}{\partial y}\right)_{\substack{\text{outer} \\ y \to o}}$$

$$f_o''(\eta) \sim a$$

$$f_1''(\eta) = 0 \qquad \text{as } \eta \to \infty$$

$$f_2''(\eta) = 0$$

From the first two boundary conditions $f_1(\eta) = 0$, $f_1'(\eta) = 0$ as $\eta \to \infty$ and the above new condition $f_1''(\eta) = 0$ as $\eta \to \infty$ we can write equation (A1) as

$$f_1(\infty) = Ag(\infty) + B\,h(\infty) + Cp(\infty) = 0$$
$$f_1'(\infty) = Ag'(\infty) + Bh'(\infty) + Cp'(\infty) = 0$$
$$f_1''(\infty) = Ag''(\infty) + Bh''(\infty) + Cp''(\infty) = 0$$

Since $g(\eta)$, $h(\eta)$ and $p(\eta)$ are three linearly independent solutions and the Wronskian does not vanish, we must have $A = B = C = 0$, or $f_1(\eta) \equiv 0$ is the unique solution.

APPENDIX B

Numerical Integration of a Third Order Nonlinear Ordinary Differential Equation with Boundary Condition at Positive and Negative Infinity

The differential equation for f_o is nonlinear and third order, and the three boundary conditions are unfortunately all at infinity. A closed form solution for the O. D. E. could not be obtained. A special numerical method was employed here for solving this particular problem.

The method is illustrated as follows:

Differential equation
$$3f''' + 2ff'' - (f')^2 = 0 \qquad \text{(B1)}$$

Boundary conditions
$$\left.\begin{aligned} f(x) &\sim \frac{a}{2}x^2 \\ f'(x) &\sim a\,x \end{aligned}\right\} \quad x \to \infty \qquad \text{(B1a)}$$

$$f'(x) = 0 \qquad x \to -\infty \qquad \text{(B1b)}$$

Procedure

1. Transform the above equation into a set of three first orders. With $f'' = u'$ we get

$$\left.\begin{aligned} v' &= -\tfrac{2}{3} fv + \tfrac{1}{3} u^2 \\ u' &= v \\ f' &= u \end{aligned}\right\} \qquad \text{(B2)}$$

2. Integration for an estimated set of initial conditions at $x = 0$.

For given initial values $f(0) = f_o$, $f'(0) = u(0) = u_o$, $f''(0) = v(0) = v_o$, integration in both negative and positive directions can easily be done by a Runge-Kutta method. A few test integrations will give u-curves of the kind shown in the accompanying sketch.

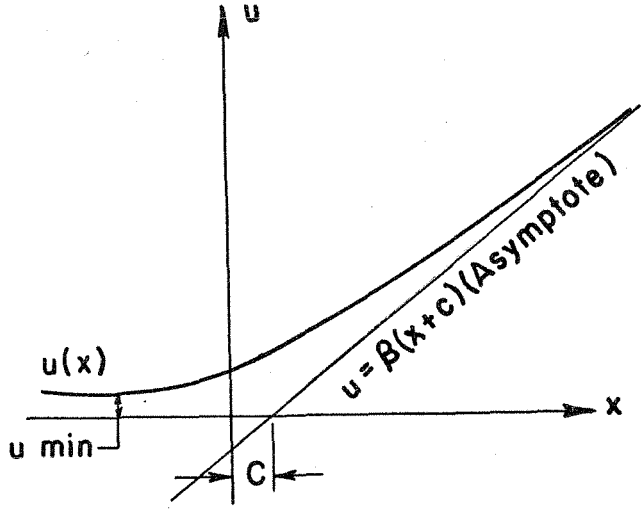

The values of u_{min}, C and β depend on the chosen initial values of f_o, u_o and v_o. They can be obtained from the results of the integration (list of the functions f, u, v) by realizing that β is identical with V(x) and $C = \left[u \frac{(x)}{\beta} - x\right]$ for large positive values of x. The problem is now to find a set of initial values such that the boundary conditions are satisfied. The boundary conditions (B1a) demand $\beta = \alpha$ and $c = 0$, while the boundary condition (B1b) requires $u_{min} = 0$ ($u_{min} = 0$ means that at the same x value $u = 0$ and $u' = v = 0$ and thus, because of the first equation of (B2), all further derivatives of u are also zero).

3. Systematic improvement of the initial values:

Let $f_o^{(i)}$, $u_o^{(i)}$, $v_o^{(i)}$, $u_{min}^{(i)}$, $c^{(i)}$, $\beta^{(i)}$ with i = 1, 2, 3, 4 be 4 sets of 6 values each, where the first three were chosen and the last three resulted from the integration.

If the first three values were reasonably estimated such that the last three values are not too far away from the desired values $u_{min} = 0$, $c = 0$, $\beta = \alpha$, then improved initial values f_o^*, u_o^*, v_o^* can be obtained from the following system of linear equations

$$\begin{bmatrix} 1 & \Delta u_{min}^{(1)} & \Delta C^{(1)} & \Delta\alpha^{(1)} \\ 1 & \Delta u_{min}^{(2)} & \Delta C^{(2)} & \Delta\alpha^{(2)} \\ 1 & " & " & " \\ 1 & " & " & \Delta\alpha^{(4)} \end{bmatrix} \begin{bmatrix} f_o^* & u_o^* & v_o^* \\ \left(\frac{\partial f_o}{\partial u_{min}}\right)^* & \left(\frac{\partial u_o}{\partial u_{min}}\right)^* & \left(\frac{\partial v_o}{\partial u_{min}}\right)^* \\ \left(\frac{\partial f_o}{\partial c}\right)^* & \left(\frac{\partial u_o}{\partial c}\right)^* & \left(\frac{\partial v_o}{\partial c}\right)^* \\ \left(\frac{\partial f_o}{\partial \beta}\right)^* & \left(\frac{\partial u_o}{\partial \beta}\right)^* & \left(\frac{\partial v_o}{\partial \beta}\right)^* \end{bmatrix}$$

$$= \begin{bmatrix} f_o^{(1)} & u_o^{(1)} & v_o^{(1)} \\ f_o^{(2)} & u_o^{(2)} & v_o^{(2)} \\ f_o^{(3)} & " & " \\ f_o^{(4)} & " & " \end{bmatrix} \qquad \text{(B3)}$$

with

$$\left.\begin{aligned} \Delta u_{min}^{(i)} &= u_{min}^{(i)} - u_{min}^* = u_{min}^{(i)} \\ \Delta C^{(i)} &= C^{(i)} - C^* = C \\ \Delta\beta &= \beta^{(i)} - \beta^* \end{aligned}\right\} \qquad \text{(B3a)}$$

One can consider f_o, u_o and v_o as functions of u_{min}, c and β. If the

set $u_{min}^{(i)}$, $c^{(i)}$, $\beta^{(i)}$ is sufficient close to the set u^*_{min}, c^*, β^*, the values of $f_o^{(i)}$, $u_o^{(i)}$ and $v_o^{(i)}$ can be approximated by the linear term of the Taylor series

$$f_o^{(i)} \approx f_o^* + \left(\frac{\partial f_o}{\partial u_{min}}\right)^* (u_{min}^{(i)} - u^*_{min}) + \left(\frac{\partial f_o}{\partial c}\right)(c^{(i)} - c^*) + \left(\frac{\partial f_o}{\partial \beta}\right)(\beta^{(i)} - \beta^*)$$

$$u_o^{(i)} \approx u_o^* + \left(\frac{\partial u_o}{\partial u_{min}}\right)^* (u_{min}^{(i)} - u^*_{min}) + \left(\frac{\partial u_o}{\partial c}\right)(c^{(i)} - c^*) + \left(\frac{\partial u_o}{\partial \beta}\right)^* (\beta^{(i)} - \beta^*)$$

$$v_o^{(i)} \approx v_o^* + \left(\frac{\partial v_o}{\partial u_{min}}\right)^* (u_{min}^{(i)} - u^*_{min}) + \left(\frac{\partial v_o}{\partial c}\right)(c^{(i)} - c^*) + \left(\frac{\partial v_o}{\partial \beta}\right)(\beta^{(i)} - \beta^*)$$

with i = 1, 2, 3, 4, then this is a system of 12 linear equations which can be written in the matrix form as (B3).

Similarly other sets of nonlinear ordinary differential equations appearing in the previous section can be solved in the same manner. This system is set up and solved by using a 7094 IBM computer. Magnitude of allowable error is of the order of 10^{-6}.

TABLE I (a)

Blasius Initial Velocity Profile

η	f_o	f_o'	f_o''
0	-.32775	.29227	.14534
.25	-.24998	.33052	.16078
.50	-.16215	.37272	.17688
.75	-.063279	.41900	.19342
1.00	.04768	.46944	.21013
1.25	.17179	.52405	.22670
1.50	.31006	.58276	.24280
1.75	.46350	.64539	.25809
2.00	.63306	.71171	.27225
2.25	.81963	.78140	.28498
2.50	1.02401	.85407	.29609
2.75	1.24688	.92930	.30546
3.00	1.48884	1.00666	.31308
3.25	1.75036	1.08570	.31902
3.50	2.03180	1.16605	.32347
3.75	2.33346	1.24733	.32664
4.00	2.65553	1.32928	.32879
4.25	2.99814	1.41167	.33018
4.50	3.36139	1.49433	.33102
4.75	3.74532	1.57715	.33150
5.00	4.14997	1.66006	.33176
5.25	4.57356	1.74302	.33189
5.50	5.02149	1.82601	.33195

TABLE I (a) Continued

η	f_o	f_o'	f_o''
5.75	5.48837	1.90900	.33198
6.00	5.97599	1.99200	.33199
6.25	6.48437	2.07500	.33199
6.50	7.01349	2.15800	.33200
6.75	7.56337	2.24100	.33200
7.00	8.13399	2.32400	.33200
-.25	-.39643	.25778	.13071
-.5	-.45693	.22683	.11702
-.75	-.51012	.19918	.10433
-1.00	-.55678	.17458	.09267
-1.25	-.59764	.15276	.08204
-1.50	-.63337	.13347	.07242
-1.75	-.66457	.11646	.06377
-2.00	-.67178	.10151	.05602
-2.25	-.71548	.08838	.04911
-2.50	-.73611	.07689	.04298
-2.75	-.75405	.06683	.037558
-3.00	-.76964	.05805	.032775
-3.25	-.78317	.05040	.028567
-3.50	-.79492	.04373	.024874
-3.75	-.80511	.037927	.02163
-4.00	-.81395	.032879	.01881
-4.25	-.82161	.028492	.01634

TABLE I (a) Continued

η	f_o	f_o'	f_o''
-4.50	-.82824	.024682	.01418
-4.75	-.83399	.021376	.01231
-5.00	-.83897	.018507	.01067
-5.25	-.84327	.016019	.00925
-5.50	-.84700	.013863	.00802
-5.75	-.85023	.011994	.00695
-6.00	-.85302	.010374	.00602
-6.25	-.85544	.00897	.00521
-6.50	-.85752	.00775	.00451
-6.75	-.85933	.00670	.00391
-7.00	-.86089	.00579	.00338

TABLE I (b)

Blasius Initial Velocity Profile

η	f_3	f_3'	f_3''
0	-.009719	-.07276	-.06486
.25	-.03006	-.09053	-.07760
.50	-.05527	-.11173	-.09231
.75	-.08626	-.13688	-.10923
1.00	-.12409	-.16655	-.12859
1.25	-.16997	-.20140	-.15071
1.50	-.22528	-.24217	-.17594
1.75	-.29161	-.28967	-.20472
2.00	-.37076	-.34486	-.23759
2.25	-.46478	-.40886	-.27525
2.50	-.57603	-.48296	-.31855
2.75	-.70723	-.56869	-.36848
3.00	-.86149	-.66785	-.42618
3.25	-1.0424	-.78253	-.49288
3.50	-1.2543	-.91515	-.56989
3.75	-1.5017	-1.0684	-.65849
4.00	-1.7904	-1.2455	-.75991
4.25	-2.1267	-1.4496	-.87527
4.50	-2.5178	-1.6843	-1.0056
4.75	-2.9718	-1.9537	-1.1518
5.00	-3.4978	-2.2616	-1.3147
5.25	-4.1062	-2.6125	-1.4951
5.50	-4.8080	-3.0107	-1.6938

TABLE I (b) Continued

η	f_3	f_3'	f_3''
5.75	-5.6158	-3.4609	-1.9115
6.00	-6.5432	-3.9681	-2.1491
6.25	-7.6051	-4.5372	-2.4075
6.50	-8.8175	-5.1736	-2.6874
6.75	-10.198	-5.8828	-2.9896
7.00	-11.765	-6.6704	-3.3151
7.25	-13.540	-7.5423	-3.6647
7.50	-15.544	-8.5048	-4.0393
7.75	-17.801	-9.5641	-4.4397
8.00	-20.335	-10.727	-4.8668
8.25	-23.173	-12.000	-5.3214
8.50	-26.344	-13.390	-5.8044
8.75	-29.879	-14.904	-6.3167
9.00	-33.808	-16.551	-6.8591
-.25	.00656	-.05795	-.05390
-.50	.01947	-.04568	-.04451
-.75	.02958	-.03558	-.03652
-1.00	.03741	-.02732	-.02977
-1.25	.04337	-.02060	-.02408
-1.50	.04782	-.01519	-.01933
-1.75	.05106	-.01087	-.01538
-2.00	.05334	-.00744	-.01212
-2.25	.05485	-.00476	-.00943

TABLE I (b) Continued

η	f_3	f_3'	f_3''
-2.50	.05577	-.00268	-.00724
-2.75	.05623	-.00110	-.00546
-3.00	.05635	.00007	-.00403

TABLE II

Initial Velocity Profile With Finite Slip

η	f_o	f_o'	f_o''	f_1	f_1'	f_1''
0	.33782	.69202	.19080	-.84571	.57922	.64136
.25	.51670	.73856	.18090	-.68023	.74713	.70045
.50	.70686	.78219	.16760	-.47101	.92864	.74990
.75	.90748	.82213	.15153	-.21498	1.1212	.78894
1.00	1.1176	.85779	.13353	.09030	1.3223	.81799
1.25	1.3360	.88881	.11456	.44667	1.5295	.83859
1.50	1.5616	.91507	.09558	.85541	1.7411	.85302
1.75	1.7931	.93668	.077512	1.3175	1.9557	.86384
2.00	2.0296	.95396	.061041	1.8335	2.1729	.87339
2.25	2.2698	.96738	.04666	2.4041	2.3924	.88339
2.50	2.5130	.97749	.03460	3.0299	2.6147	.89479
2.75	2.7583	.98488	.02489	3.7117	2.8400	.90771
3.00	3.0052	.99011	.01736	4.4502	3.0686	.92168
3.25	3.2532	.99372	.01174	5.2463	3.3008	.93589
3.50	3.5020	.99612	.00769	6.1009	3.5365	.94945
3.75	3.7512	.99767	.00489	7.0148	3.7754	.96165
4.00	4.0008	.99864	.00301	7.9889	4.0172	.97201
4.25	4.2505	.99923	.00179	9.0236	4.2613	.98034
4.50	4.5004	.99958	.00104	10.120	4.5072	.98671
4.75	4.7503	.99978	.00058	11.277	4.7545	.99135
5.00	5.0002	.99989	.00031	12.497	5.0028	.99458
5.25	5.2502	.99994	.00016	13.779	5.2517	.99673
5.50	5.5002	.99998	.00008	15.123	5.5011	.99810

TABLE II Continued

η	f_o	f_o'	f_o''	f_1	f_1'	f_1''
5.75	5.7502	.99999	0.00004	16.529	5.7507	.99894
6.00	6.0002	1.0000	0.00002	17.998	6.0005	.99943
6.25	6.2502	1.0000	0.00000	19.530	6.2504	.99971
6.50	6.5002	1.0000	0.00000	21.123	6.5003	.99986
6.75	6.7502	1.0000	0.00000	22.780	6.7503	.99994
7.00	7.0002	1.0000	0.00000	24.499	7.0003	.99998
7.25	7.2502	1.0000	0.00000	26.280	7.2503	1.0000
7.50	7.5002	1.0000	0.00000	28.124	7.5003	1.0000
7.75	7.7502	1.0000	0.00000	30.030	7.7503	1.0000
8.00	8.0002	1.0000	0.00000	31.999	8.0003	1.0000
-.25	.17085	.64347	.19694	-.97115	.42710	.57451
-.50	.01617	.59387	.19923	-1.0607	.2924	.50254
-.75	-.12607	.54416	.19784	-1.1189	.17600	.42849
-1.00	-.25597	.49522	.19315	-1.1503	.07807	.35537
-1.25	-.37381	.44782	.18567	-1.1594	-.00197	.28579
-1.50	-.48006	.40257	.17600	-1.1507	-.06529	.22182
-1.75	-.57532	.35995	.16475	-1.1280	-.11347	.16483
-2.00	-.66028	.32028	.15249	-1.0950	-.14835	.11554
-2.25	-.73572	.28375	.13974	-1.0548	-.17190	.07411
-2.50	-.80242	.25042	.12692	-1.0099	-.18604	.04025
-2.75	-.86119	.22026	.11437	-.96240	-.19260	.01336
-3.00	-.91281	.19318	.10236	-.91406	-.19324	-.00733
-3.25	-.95803	.16902	.09106	-.86616	-.18938	-.02270
-3.50	-.99755	.14759	.08058	-.81965	-.18225	-.033617

TABLE II Continued

η	f_o	f_o'	f_o''	f_1	f_1'	f_1''
-3.75	-1.032	.12866	.07097	-.77522	-.17287	-.04088
-4.00	-1.0621	.11202	.062268	-.73333	-.16205	-.04525
-4.25	-1.0882	.09745	.05443	-.69426	-.15044	-.04736
-4.50	-1.1109	.08473	.04744	-.65814	-.13851	-.04776
-4.75	-1.1307	.07366	.04124	-.62499	-.12666	-.04691
-5.00	-1.1479	.06405	.03576	-.59478	-.11513	-.04516
-5.25	-1.1628	.05572	.03095	-.56738	-.10412	-.04282
-5.50	-1.1759	.04852	.02674	-.54266	-.09375	-.04011
-5.75	-1.1872	.04231	.02307	-.52045	-.08408	-.03720
-6.00	-1.1971	.03695	.01987	-.50056	-.07515	-.03422
-6.25	-1.2057	.03233	.01710	-.48281	-.06697	-.03126
-6.50	-1.2133	.02836	.01470	-.46701	-.05951	-.02840
-6.75	-1.2200	.02495	.01263	-.45299	-.05275	-.02567
-7.00	-1.2258	.02202	.01084	-.44058	-.04666	-.02311
-7.25	-1.2310	.01951	.00929	-.42961	-.04118	-.02072
-7.50	-1.2356	.01736	.00796	-.41994	-.03628	-.01853
-7.75	-1.2397	.01551	.00682	-.41142	-.03190	-.01651
-8.00	-1.2434	.01393	.00584	-.40394	-.02800	-.01468

TABLE II Continued

η	f_2	f_2'	f_2''
0	0.69900	1.03667	1.21641
.25	0.99891	1.37371	1.48386
.50	1.39167	1.78045	1.77351
.75	1.89539	2.26218	2.08376
1.00	2.52944	2.82405	2.41467
1.25	3.31453	3.47139	2.76803
1.50	4.27276	4.21017	3.14667
1.75	5.42780	5.04706	3.55330
2.00	6.80507	5.98927	3.98922
2.25	8.43181	7.04403	4.45328
2.50	10.33702	8.21794	4.94163
2.75	12.55117	9.51637	5.44822
3.00	15.10589	10.94298	5.96592
3.25	18.03350	12.49968	6.48784
3.50	21.36660	14.18678	7.00842
3.75	25.13770	16.00348	7.52413
4.00	29.37902	17.94832	8.03350
4.25	34.02240	20.01972	8.53678
4.50	39.39931	22.21631	9.03526
4.75	45.24090	24.53710	9.53070
5.00	51.67816	26.98154	10.02474
5.25	58.74196	29.54946	10.51867
5.50	66.46319	32.24094	11.01330
5.75	74.87274	35.05620	11.50898

TABLE II Continued

η	f_2	f_2'	f_2''
6.00	84.00162	37.99552	12.00577
6.25	93.88086	41.05916	12.50354
6.50	104.54158	44.24735	13.00208
6.75	116.01493	47.56025	13.50117
7.00	128.33210	50.99797	14.00063
7.25	141.52431	54.56058	14.50032
7.50	155.62280	58.24814	15.00015
7.75	170.65879	62.06066	15.50005
8.00	186.66354	65.99817	16.00000
-0.25	0.475259	0.76343	0.97382
-0.50	0.31251	0.54745	0.75887
-0.75	0.19736	0.38152	0.57362
-1.00	0.11821	0.25810	0.41880
-1.25	0.06539	0.16964	0.29361
-1.50	0.03107	0.10900	0.19588
-1.75	0.00912	0.06968	0.12239
-2.00	0.00507	0.04609	0.06937

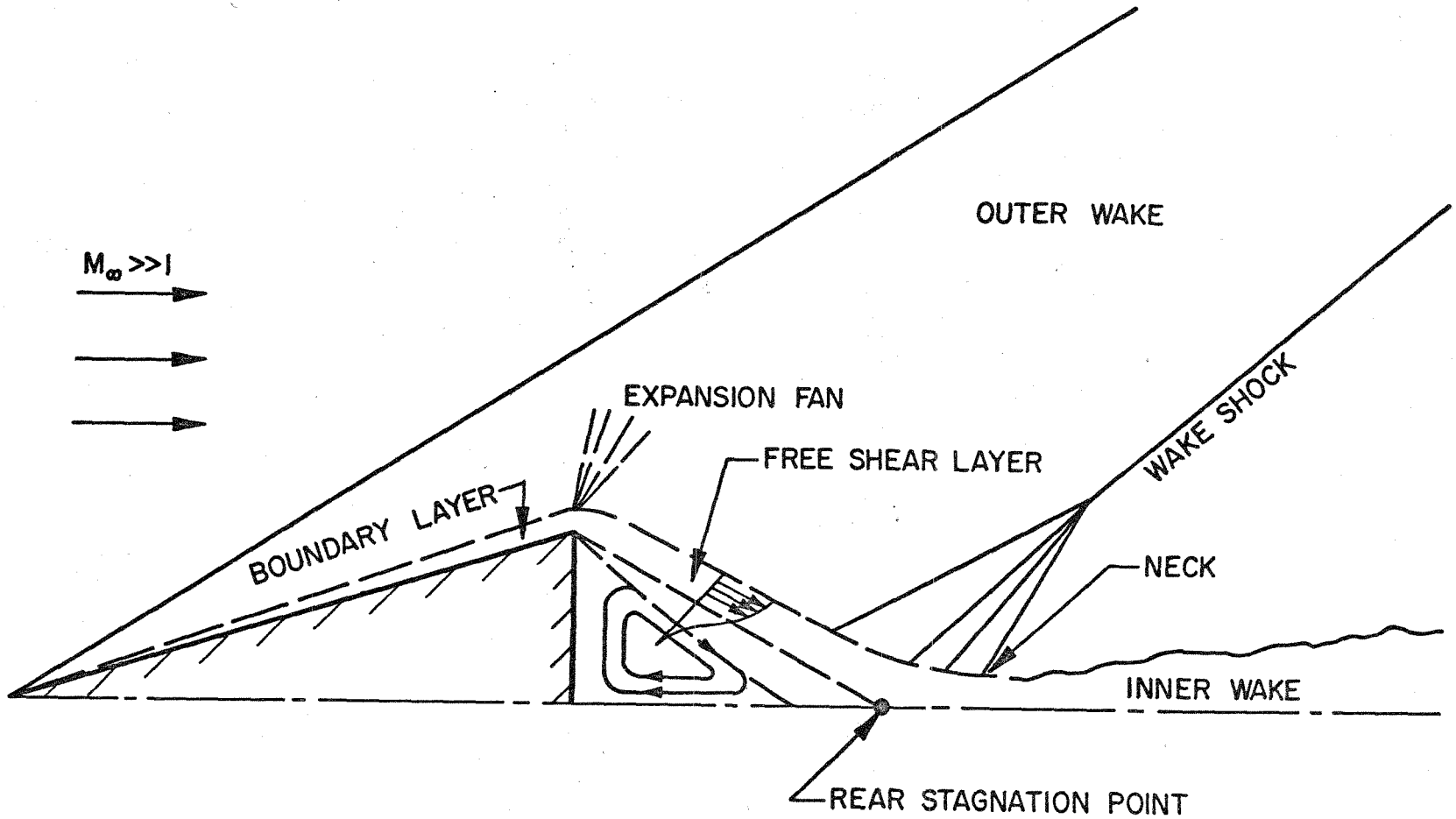

FIGURE 1 SCHEMATIC DRAWING OF HYPERSONIC WAKE

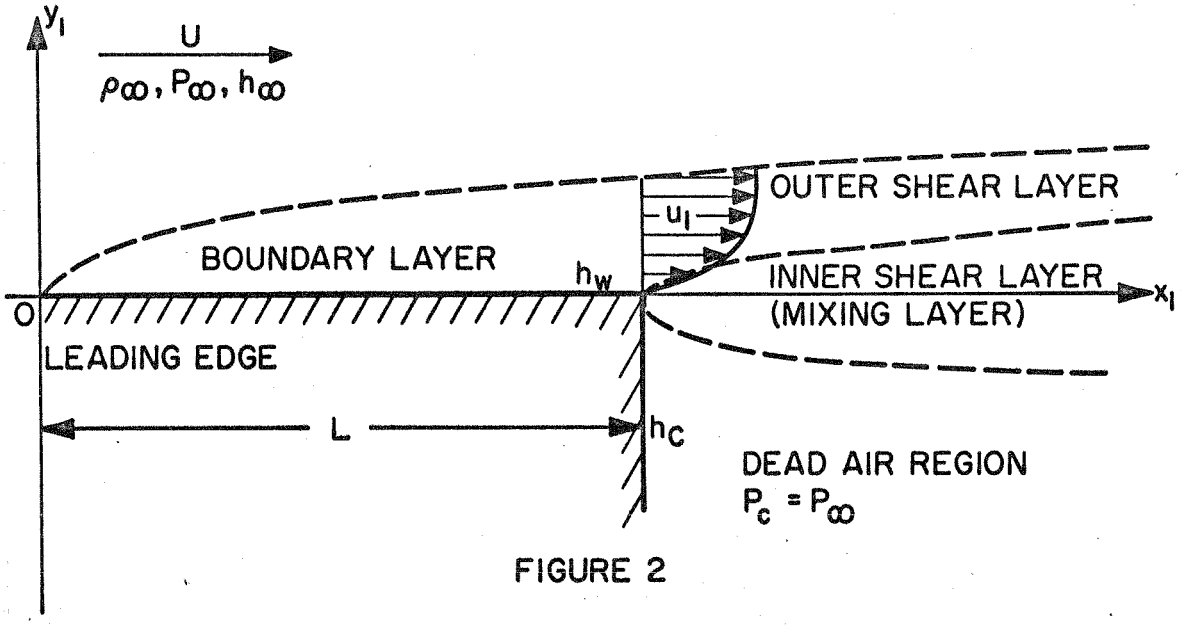

FIGURE 2

SCHEMATIC DRAWING OF THE SIMPLIFIED BASE FLOW

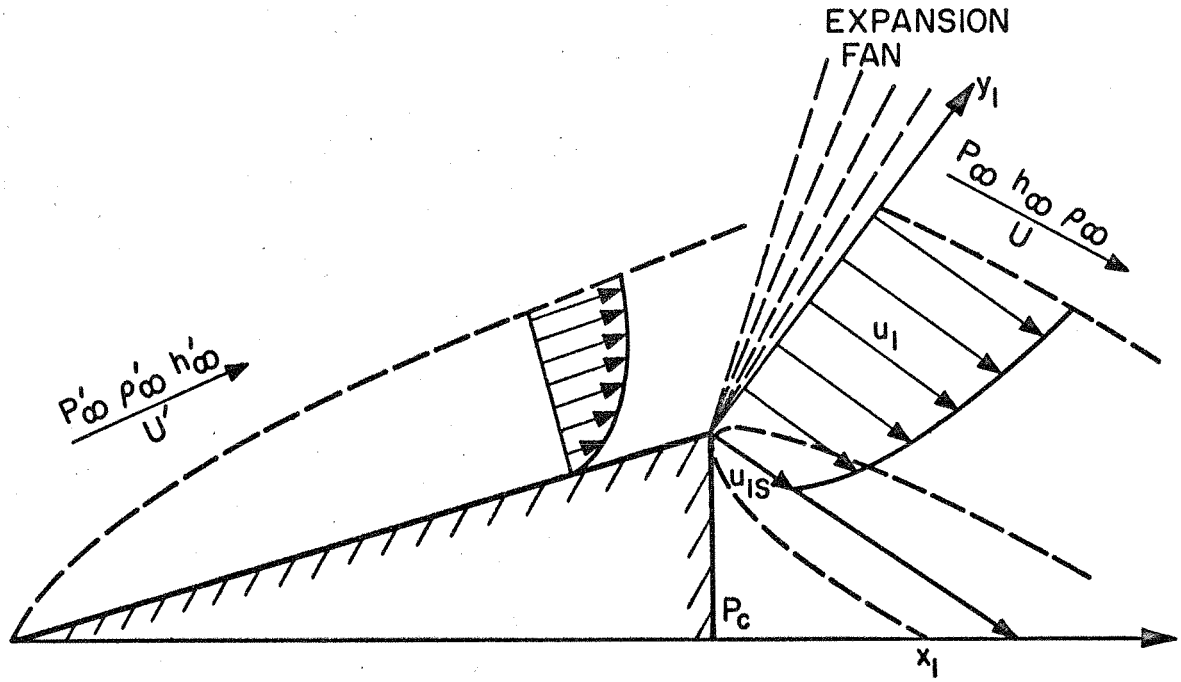

FIGURE 3

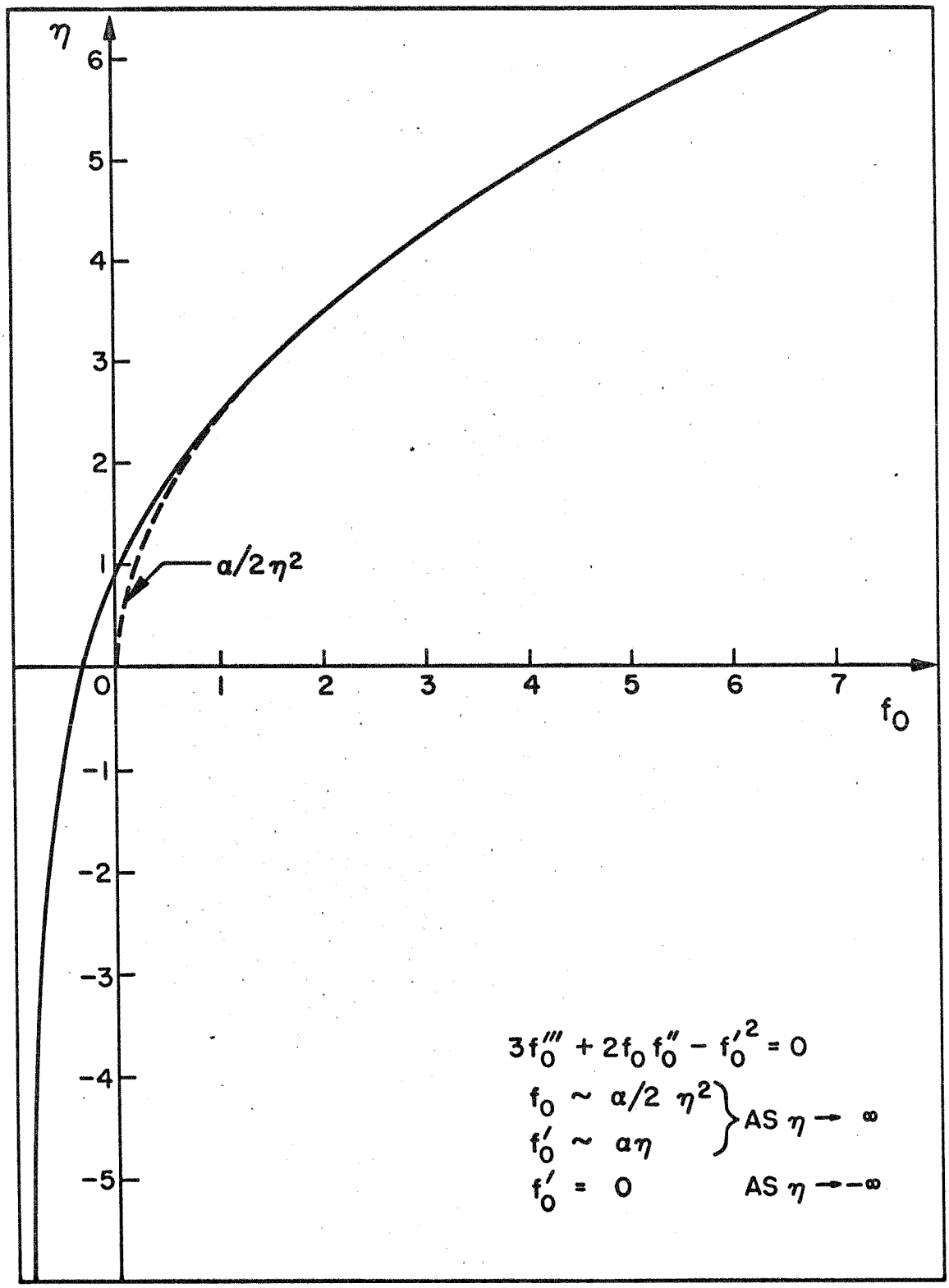

FIGURE 4A f_0 vs η

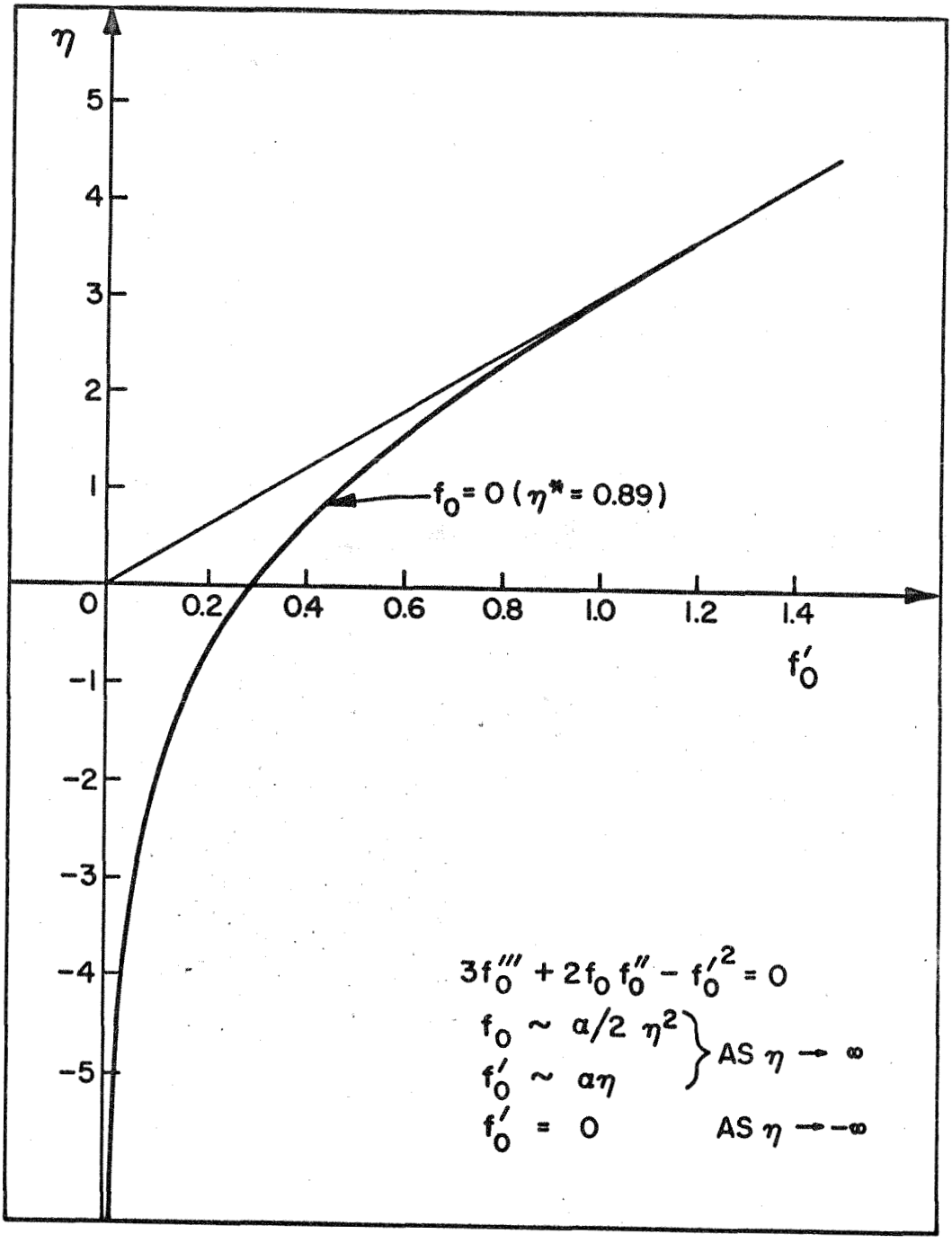

FIGURE 4B f'_0 vs η

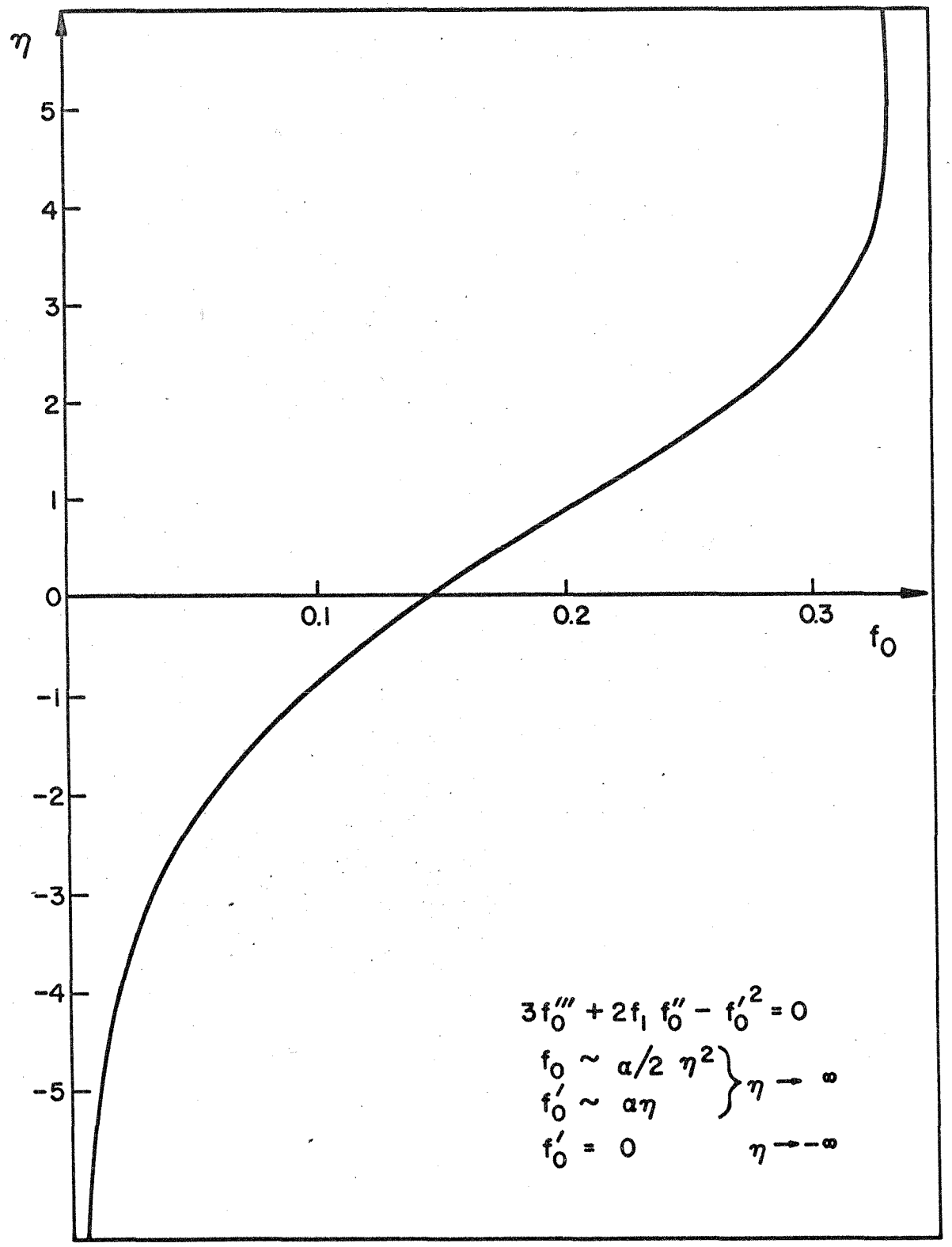

FIGURE 4C f_0'' vs η

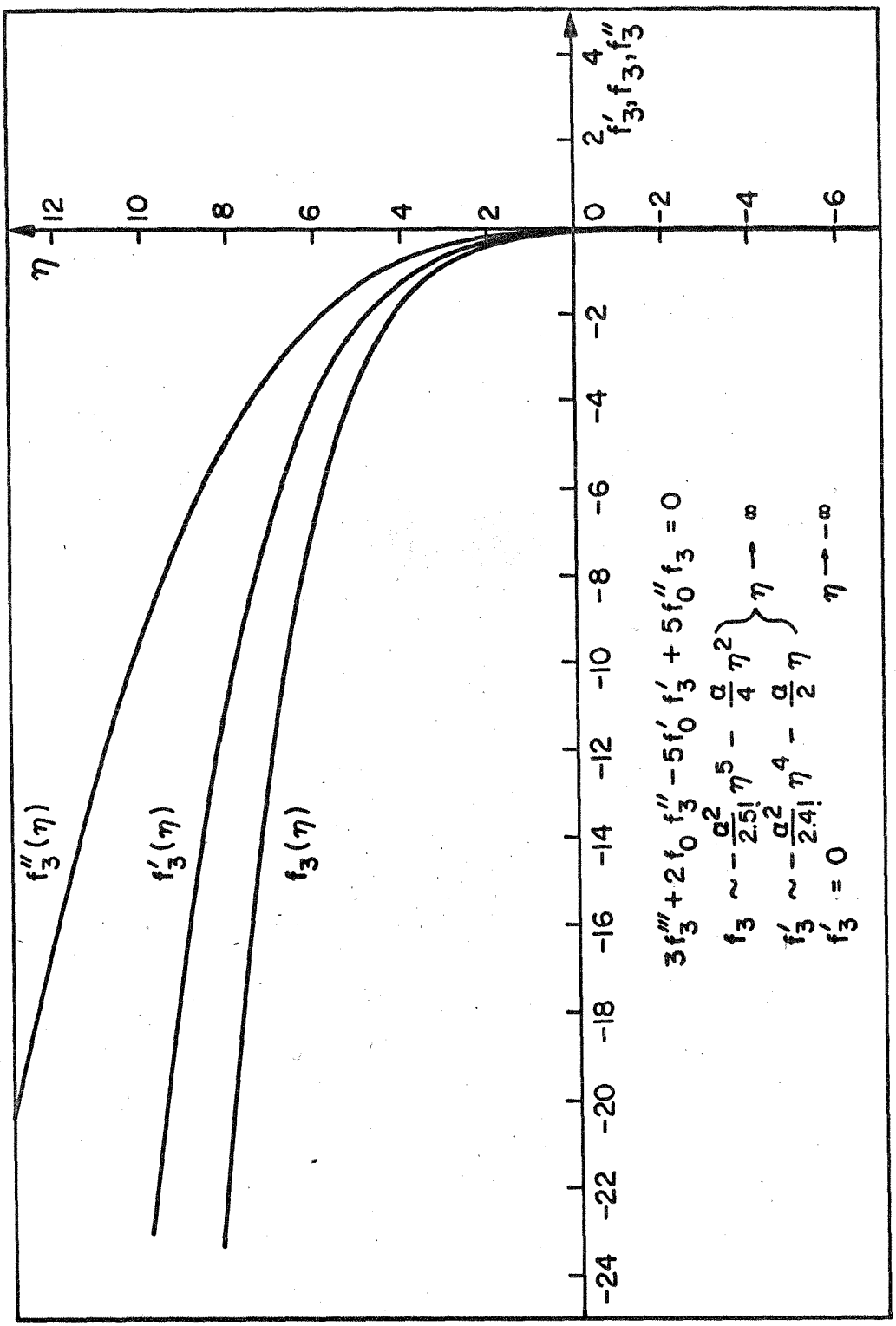

FIGURE 4D f_3, f'_3, f''_3 vs η

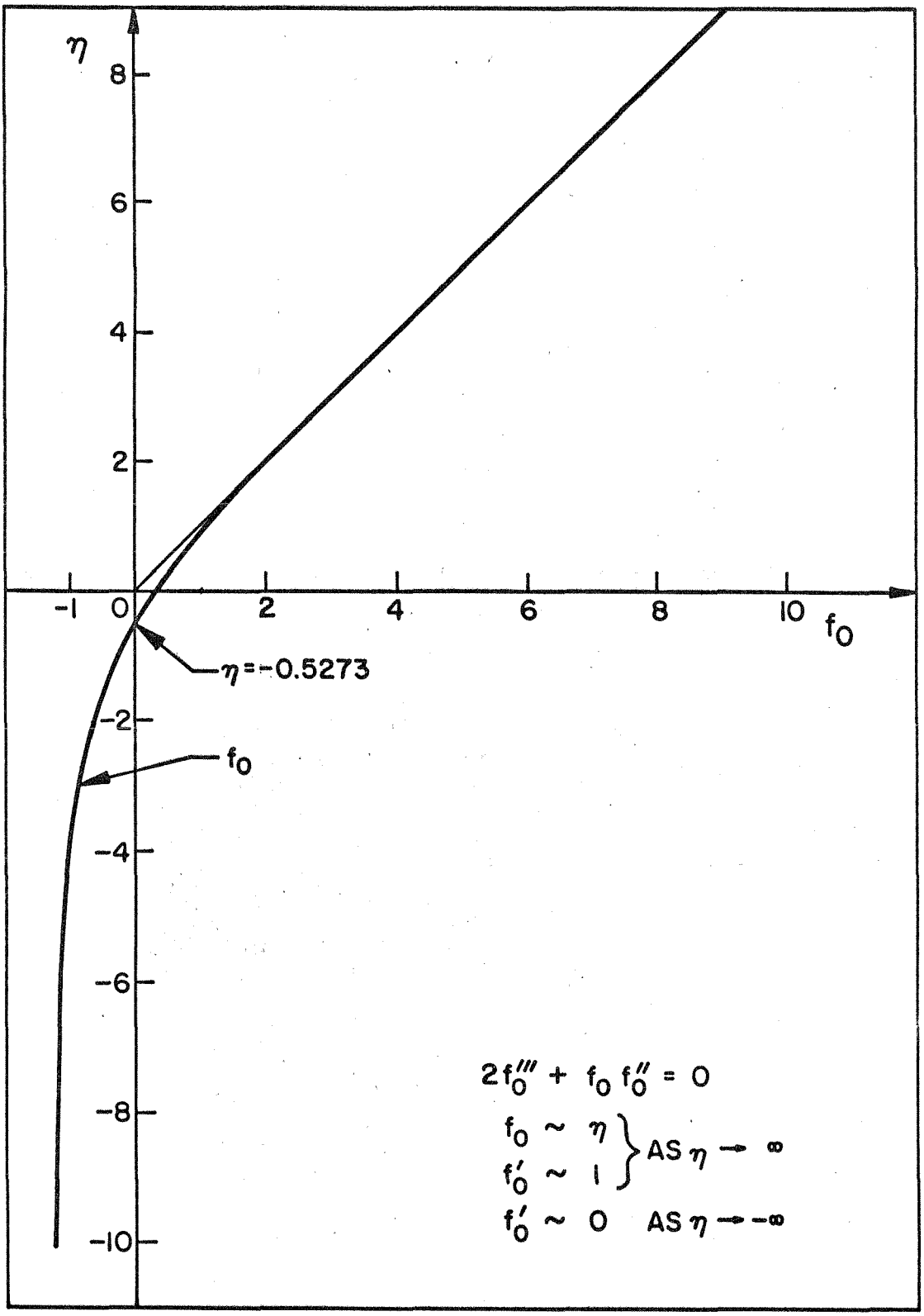

FIGURE 5A f_0 vs η

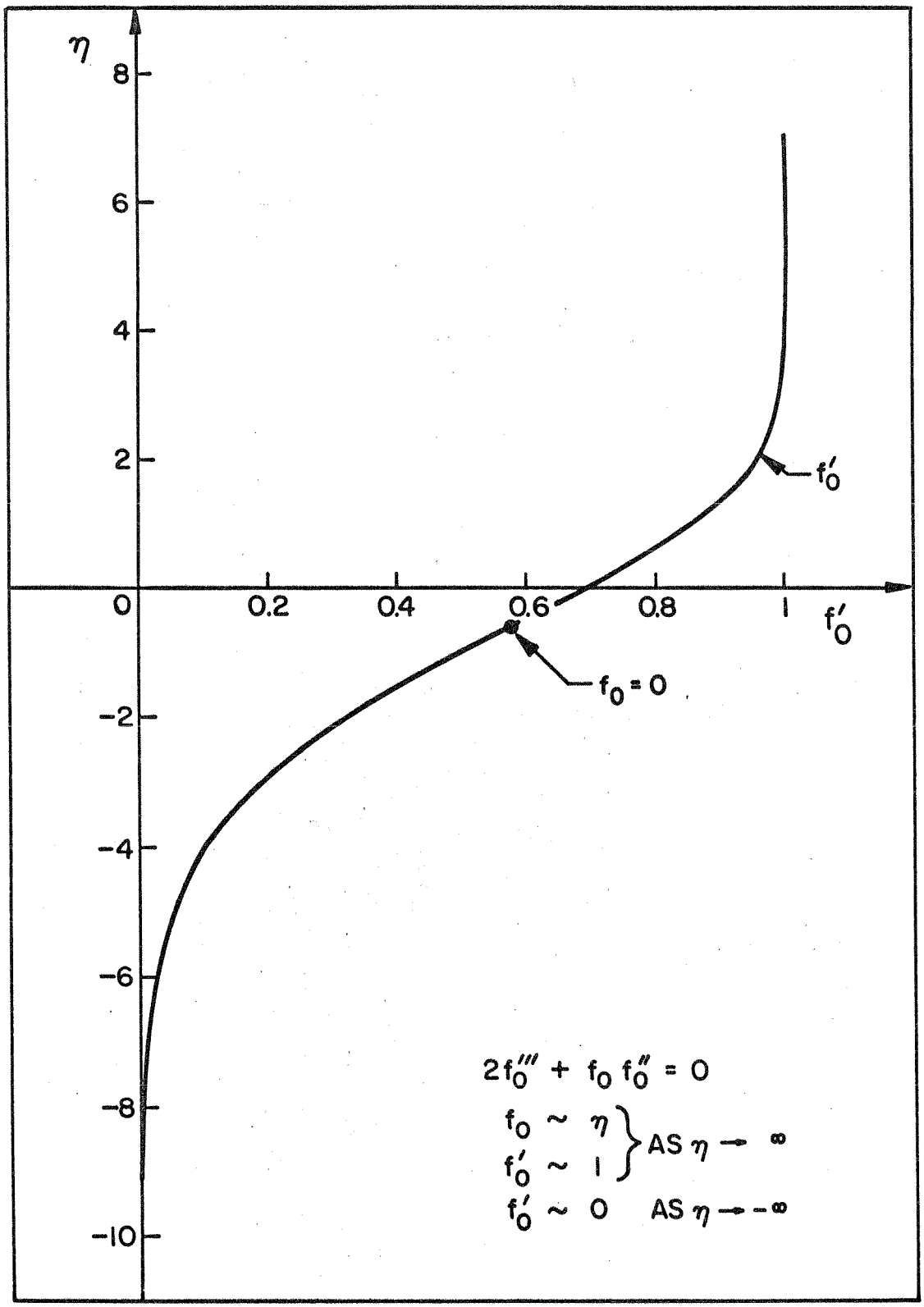

FIGURE 5B f_0' vs η

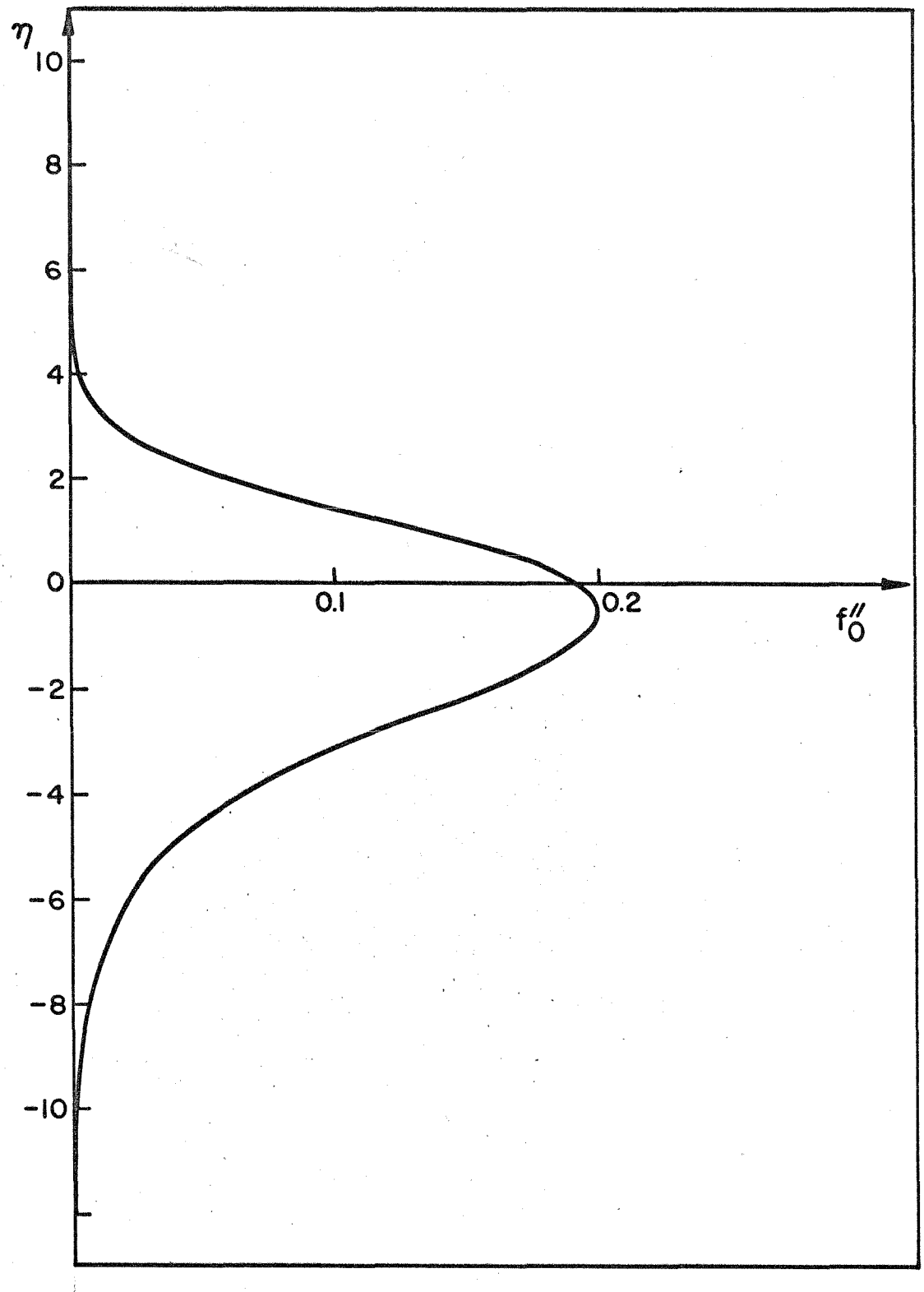

FIGURE 5C f_0'' vs η

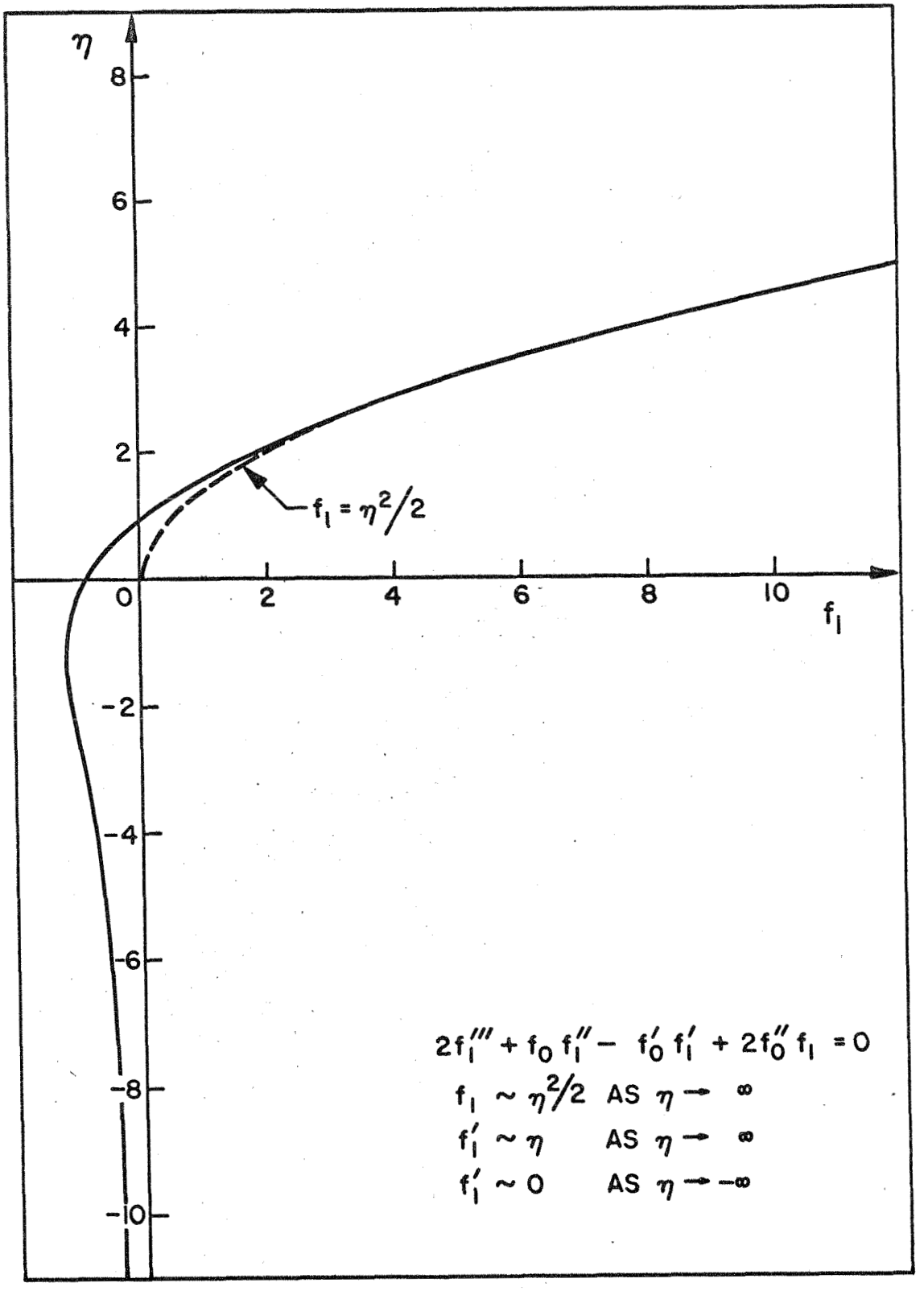

FIGURE 5D f_i vs η

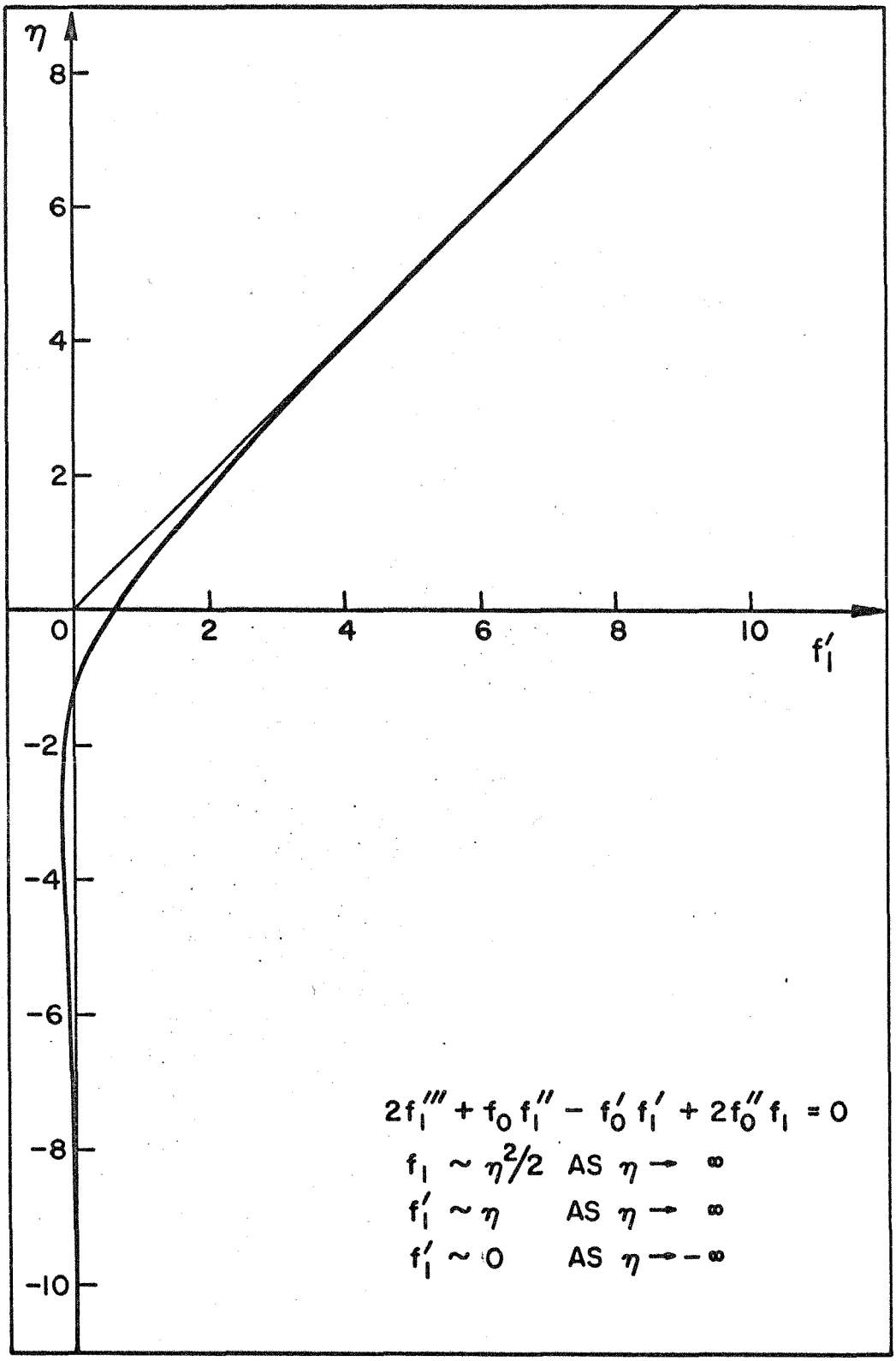

FIGURE 5E f_1' vs η

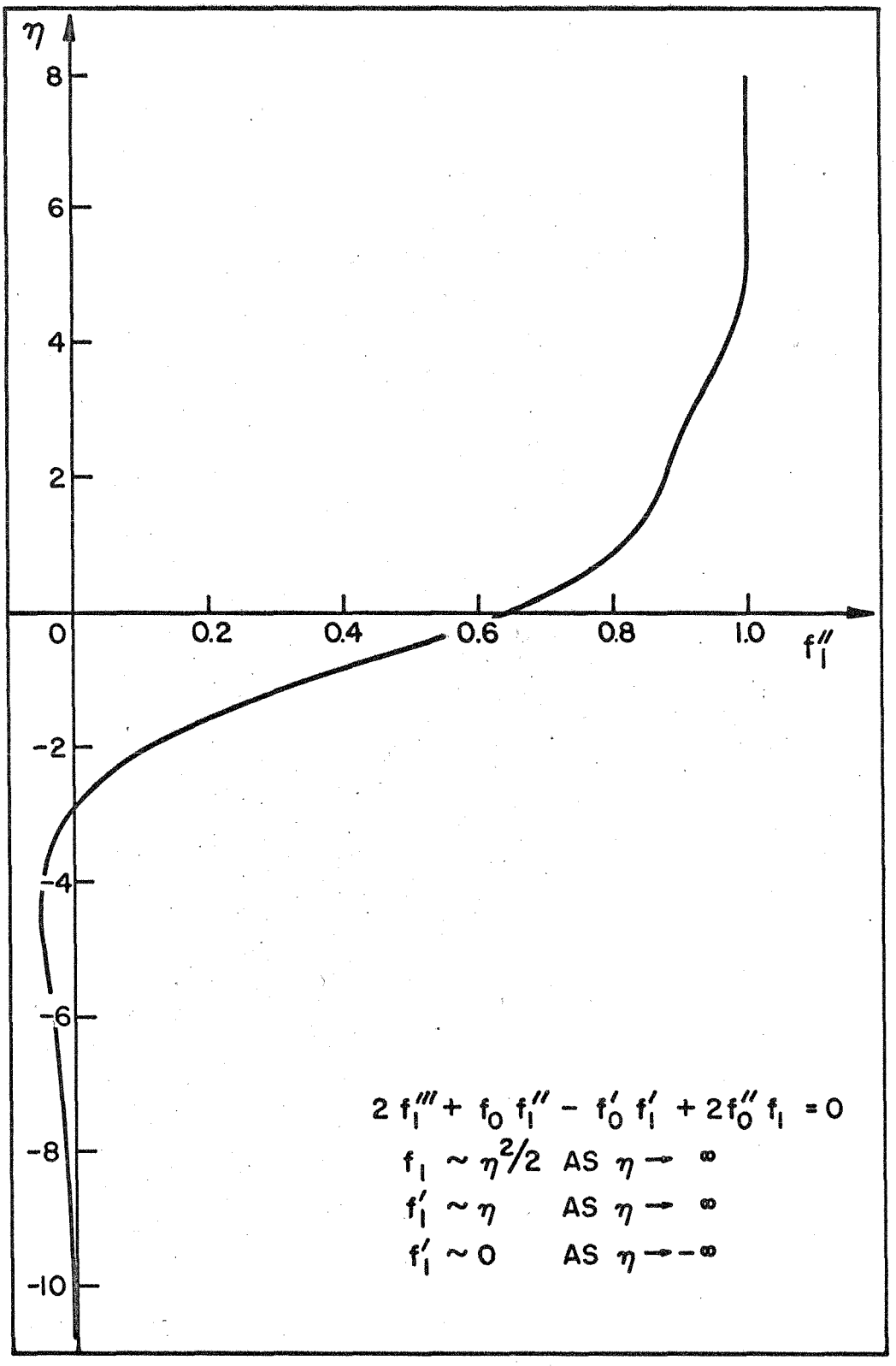

FIGURE 5F f_1'' vs η

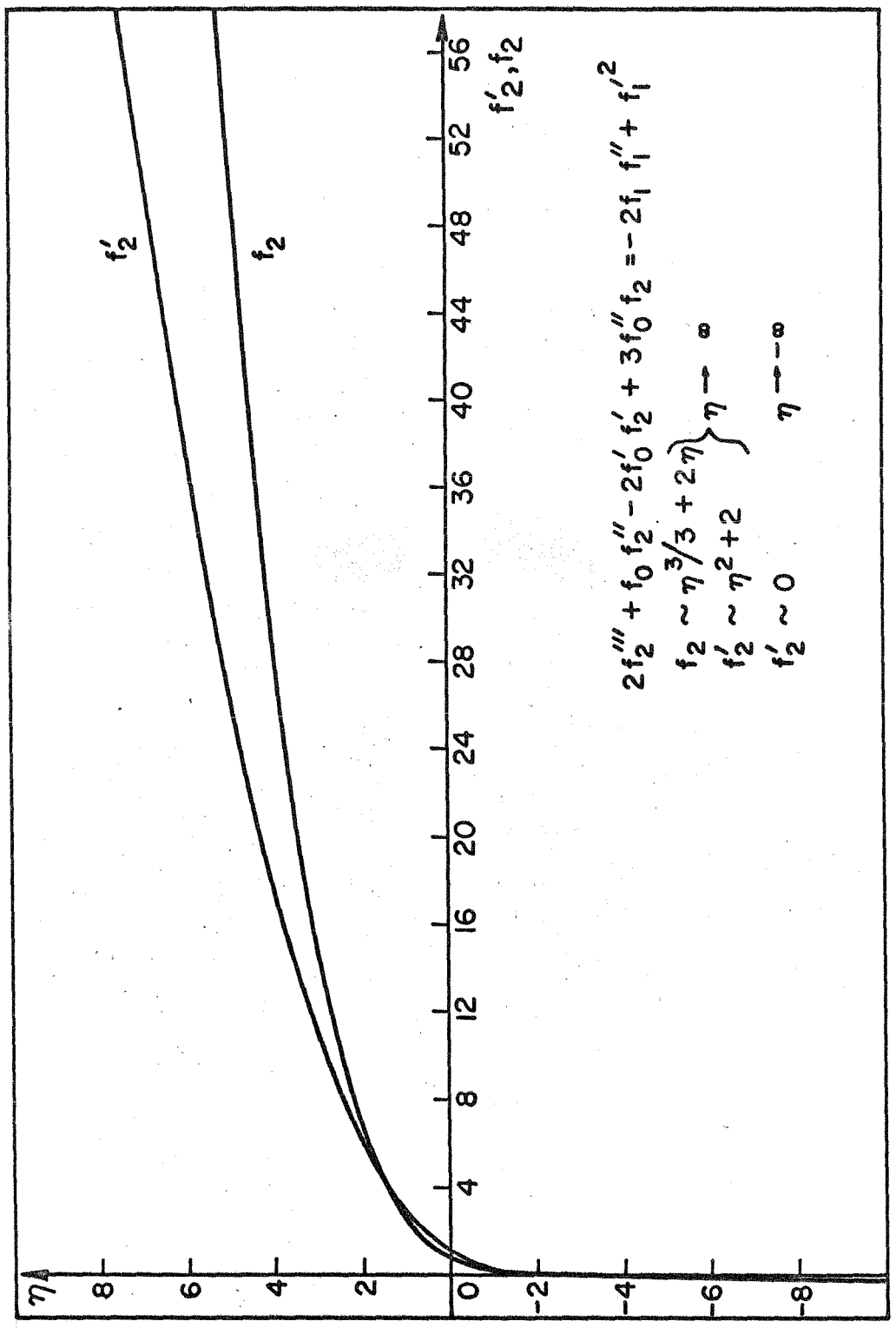

FIGURE 5G f_2, f_2' vs η

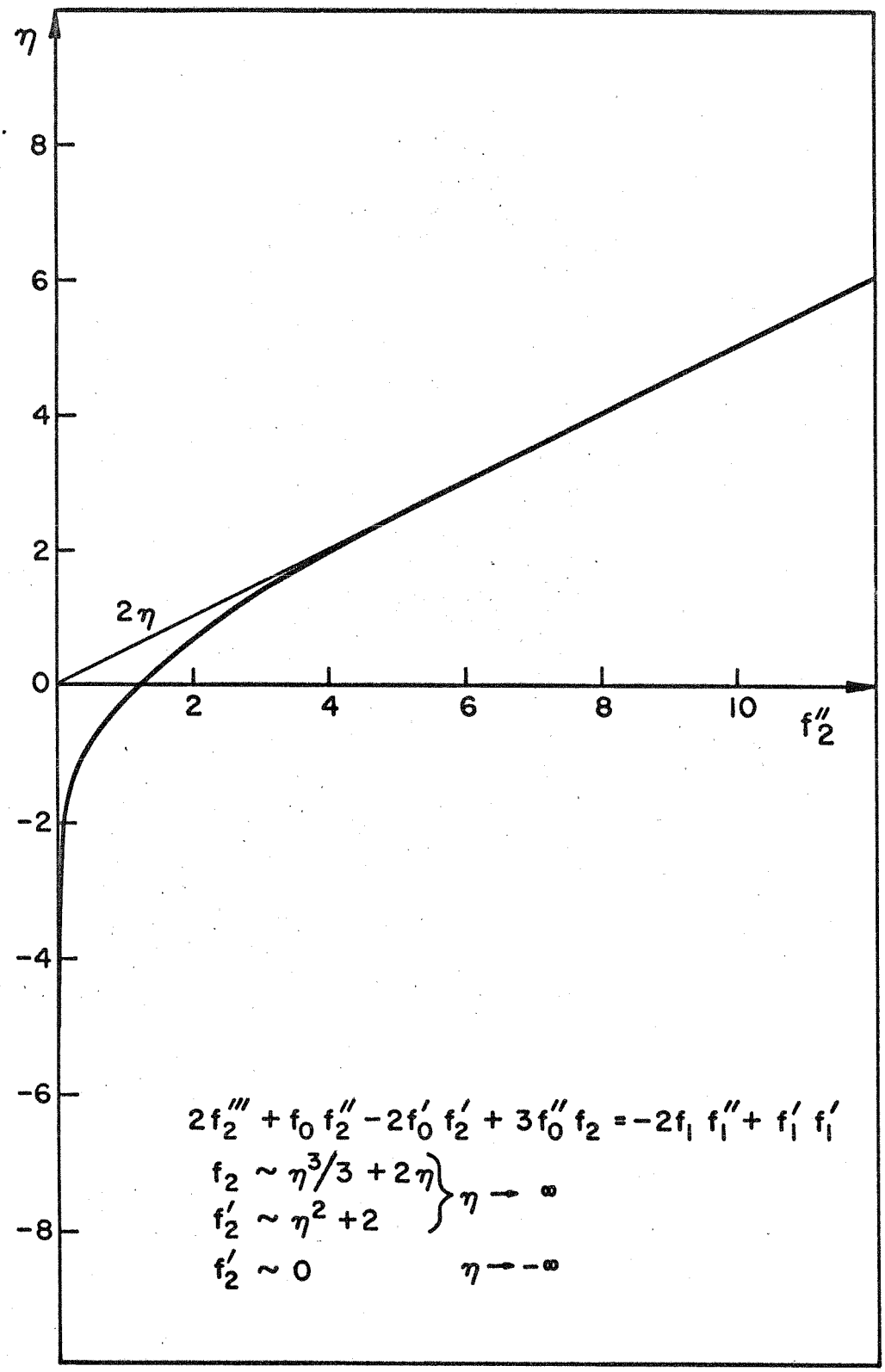

FIGURE 5H f_2'' vs η

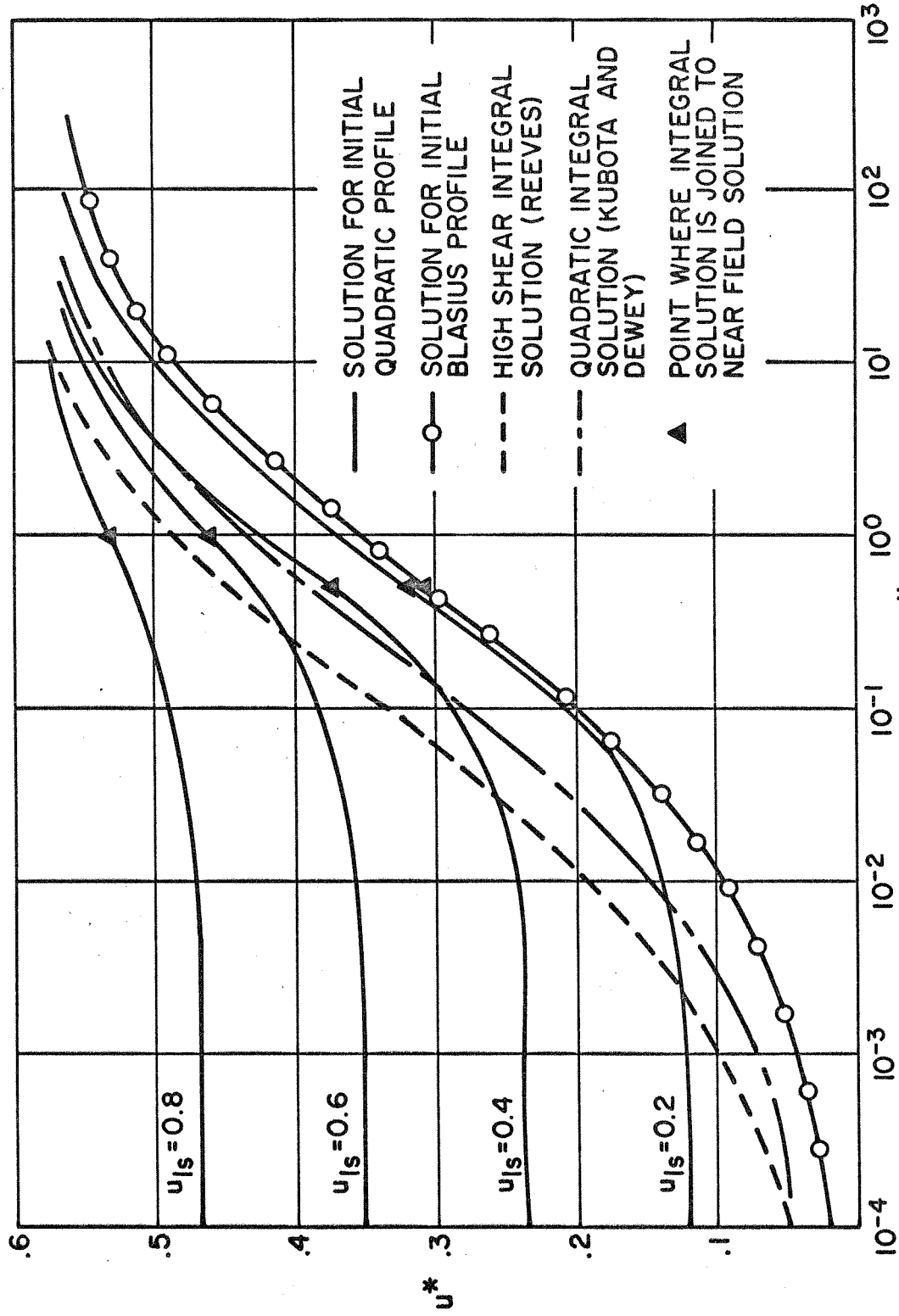

FIGURE 6 GROWTH OF VELOCITY ON DIVIDING STREAMLINE

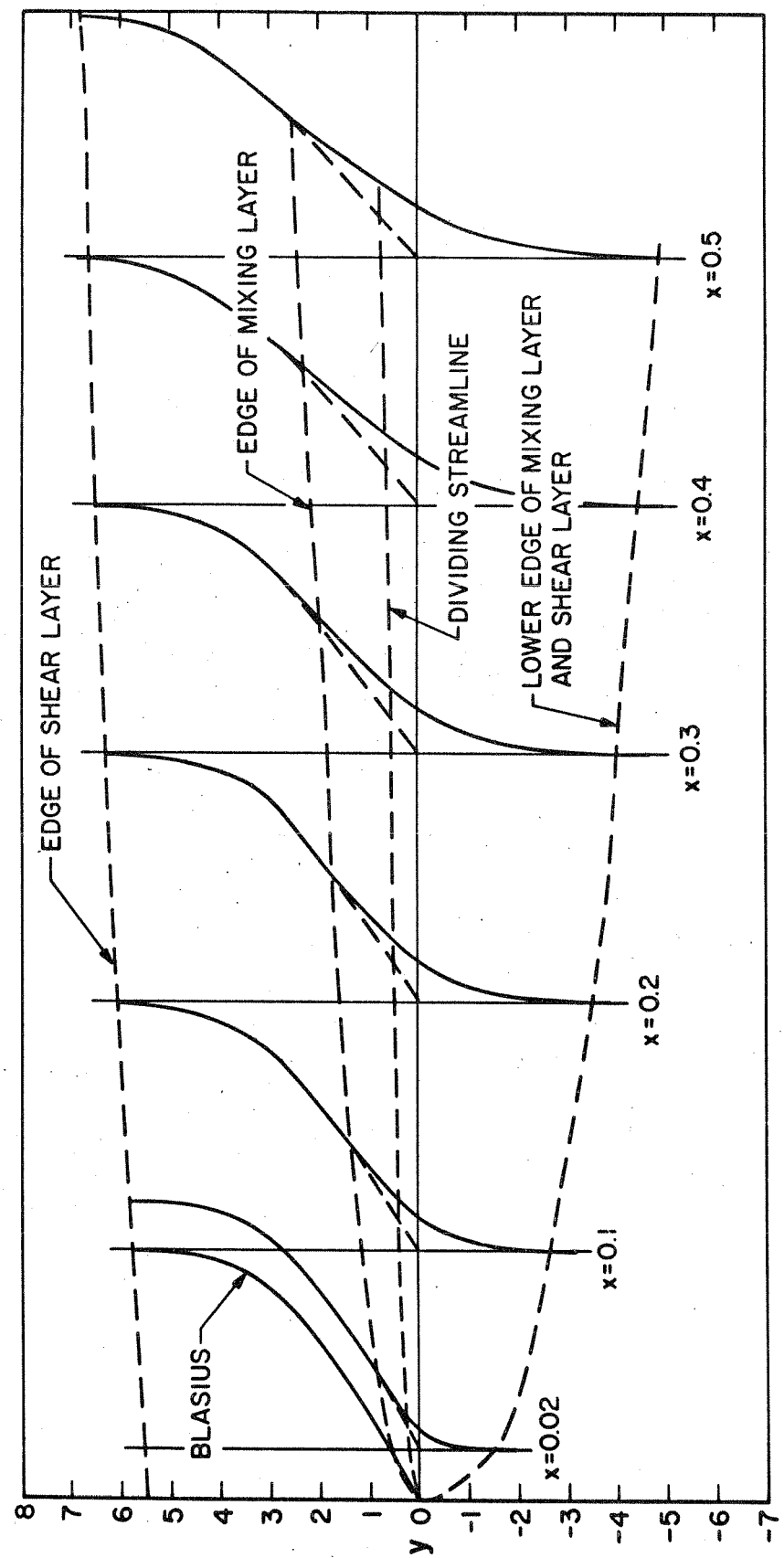

FIG. 7. GROWTH OF THE MIXING LAYER FROM NEAR FIELD SOLUTION (BLASIUS INITIAL VELOCITY PROFILE)

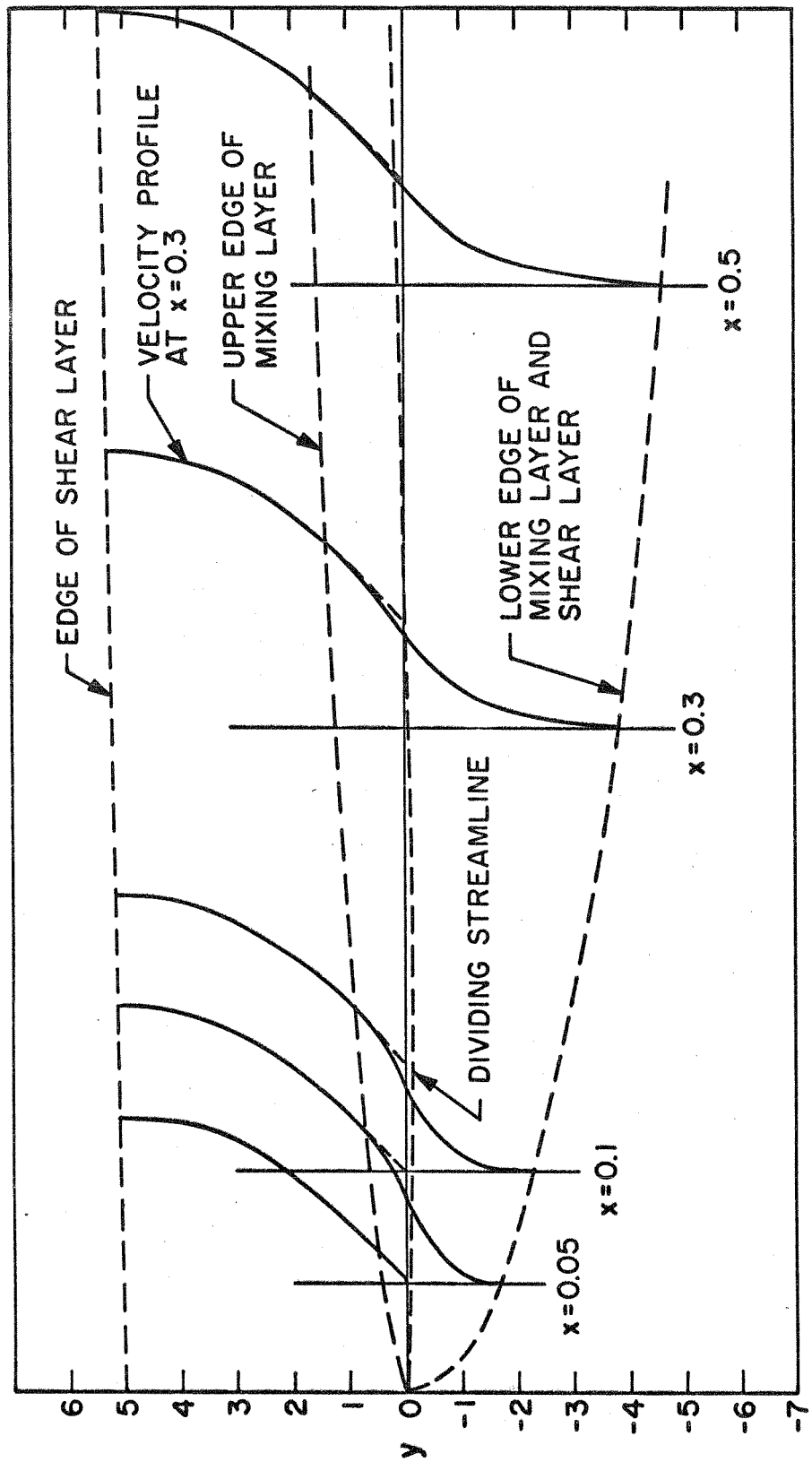

FIGURE 8 GROWTH OF THE MIXING LAYER FROM NEAR FIELD SOLUTION
(FINITE SLIP INITIAL VELOCITY PROFILE, QUADRATIC, $u_{ls} = 0.4$)